



The transcription factor HOXB7 regulates ERK kinase activity and thereby stimulates the motility and invasiveness of pancreatic cancer cells

Received for publication, December 15, 2016, and in revised form, August 29, 2017. Published, Papers in Press, September 14, 2017, DOI 10.1074/jbc.M116.772780

Makiko Tsuboi[‡], Keisuke Taniuchi^{‡§1}, Takahiro Shimizu[¶], Motoaki Saito[¶], and Toshiji Saibara^{‡§}

From the Departments of [‡]Gastroenterology and Hepatology, [§]Endoscopic Diagnostics and Therapeutics, and [¶]Pharmacology, Kochi Medical School, Kochi University, Nankoku, Kochi 783-8505, Japan

Edited by Alex Tokar

HOX genes encode transcription factors that function as sequence-specific transcription factors that are involved in cellular proliferation, differentiation, and death. The aim of this study was to investigate the role of a HOX family protein, HOXB7, in the motility and invasiveness of pancreatic cancer cells. We previously identified a *HOXB7* transcript that is one of a number of transcripts that are preferentially translated in membrane protrusions in pancreatic cancer cells. Immunocytochemistry showed that HOXB7 was localized to the cell protrusions of migrating pancreatic cancer cells. Knockdown of HOXB7 by transfection with *HOXB7*-specific siRNA decreased these protrusions and inhibited the motility and invasiveness of the cells. Transfection of a HOXB7-rescue construct into the HOXB7-knockdown cells restored peripheral actin structures in cell protrusions and abrogated the HOXB7 knockdown-induced decrease in cell protrusions. It is generally accepted that the Rho family of GTPases regulate the organization of actin filaments and contribute to the formation of cell protrusions. The levels of the active Rho GTPases were not influenced by HOXB7 in the cells; however, HOXB7 knockdown decreased the level of phosphorylated ERK1/2. This inactivation of ERK1/2 decreased cell protrusions, thereby inhibiting the invasiveness of pancreatic cancer cells. Further investigation showed that HOXB7/ERK1/2 signaling selectively stimulated JNK and HSP27 phosphorylation and thereby increased the motility and invasiveness of pancreatic cancer cells. These results suggested that HOXB7 stimulates ERK1/2 phosphorylation and provided evidence that HOXB7, besides its role in transcriptional regulation, also promotes cell motility and invasiveness.

In humans, there are at least 39 homeobox (*HOX*) genes that are organized into four clusters, A, B, C, and D, which are located on chromosomes 7, 17, 2, and 12, respectively (1). *HOX* genes encode transcription factors that are characterized by a highly conserved trihelical homeodomain that binds to specific

DNA sequences (1). The functions of homeodomain-containing proteins are diverse, including roles as classical regulators of transcription and novel roles outside of transcriptional regulation (1, 2). An example of a novel role for HOX proteins is that of human proline-rich homeodomain protein, which interacts with eIF4E to inhibit the eIF4E-dependent nuclear-cytoplasmic transport of mRNA (3). *HOX* genes are functionally important in anteroposterior patterning during embryogenesis, homeostasis in adult tissues, cell-to-cell interactions, and cell-to-extracellular matrix interactions (2). HOXB7, a member of the HOX family of proteins, plays a role in tumorigenesis. Overexpression of HOXB7 has frequently been reported in melanoma, ovarian, and breast cancer cell lines, as well as in primary tumors (4, 5). Overexpression of HOXB7 in breast cancer cells increases cell proliferation and angiogenesis by up-regulating basic fibroblast growth factor (6). Furthermore, overexpression of HOXB7 in breast cancer cells induces epithelial-mesenchymal transition, a critical step for metastasis (7). In mice carrying both *HOXB7* and *HER-2/neu* transgenes, once breast cancer appears, the cancer cells grow quickly, and metastasis to the lungs occurs at a high frequency (8). These results indicated a potential oncogenic role for HOXB7.

Pancreatic ductal adenocarcinoma (PDAC)² is among the deadliest of cancers, because PDAC cells easily invade surrounding tissues, and they metastasize at an early stage (9). HOXB7 status was investigated in a large cohort of patients with PDAC; the results showed that overexpression of HOXB7 is correlated with invasive phenotype, lymph node metastasis, and worse survival outcomes, but no influence on cell proliferation or viability was detected (10). HOXB7 is overexpressed in PDAC, as determined from published microarray data (11). We recently reported that insulin-like growth factor-2 mRNA-binding protein 3 (IGF2BP3) and IGF2BP3-bound mRNAs are localized in cytoplasmic RNA granules that accumulate in membrane protrusions of PDAC cells (12). Further investigations revealed that IGF2BP3-bound mRNAs, such as ADP-ribosylation factor 6 (*ARF6*) and Rho guanine nucleotide exchange factor 4 (*ARHGEF4*), are subsequently translated in the cell protrusions; in turn, these locally translated proteins

This study was supported by Grants-in-Aid for Scientific Research (KAKENHI) 24591013 and 15K14396. The authors declare that they have no conflicts of interest with the contents of this article.

This article contains supplemental Table S1 and Figs. S1–S3.

¹To whom correspondence should be addressed: Dept. of Endoscopic Diagnostics and Therapeutics, Kochi Medical School, Kochi University, Kohasu, Oko-cho, Nankoku, Kochi 783-8505, Japan. Tel.: 81-88-880-2338; Fax: 81-88-880-2338; E-mail: ktaniuchi@kochi-u.ac.jp.

²The abbreviations used are: PDAC, pancreatic ductal adenocarcinoma; KRAS, KRas proto-oncogene, GTPase; HRAS, HRas proto-oncogene, GTPase; RAF, rapidly accelerated fibrosarcoma; NRAS, NRas proto-oncogene, GTPase; APC, adenomatous polyposis coli; CRIB domain, Cdc42/Rac interactive binding domain; GO, gene ontology; miR, microRNA.

HOXB7 promotes cell motility and invasion

influence the invasiveness and metastatic properties of the PDAC cells (12, 13). Interestingly, *HOXB7* mRNA is one of the IGF2BP3-bound transcripts in PDAC cells (12). Thus, our previous reports suggest that the local translation of *HOXB7* mRNA in protrusions may be associated with cell invasion and metastasis. These findings suggest novel roles for HOXB7 outside of transcriptional regulation in the nucleus of PDAC cells.

In the present study, we elucidated the detailed functions of HOXB7 accumulated in the cell protrusions of PDAC cells in the formation of membrane protrusions, resulting in increases in the motility and invasiveness of the PDAC cells.

Results

Subcellular localization of HOXB7 in PDAC cells

We used immunocytochemistry to determine the subcellular localization of HOXB7 in two types of cultured PDAC cells: a moderately differentiated PDAC cell line (S2-013) (14) and a poorly differentiated PDAC cell line (PANC-1) (15). When suspended S2-013 cells attach to an immobilized fibronectin substrate, nascent membrane protrusions form (*de novo* formation of actin patches at the cell periphery), and these protrusions promote cell motility as they mature (16, 17). In S2-013 and PANC-1 cells cultured on fibronectin, HOXB7 was mainly localized to the cytoplasm of the cell bodies and the nucleus (Fig. 1A). In addition, it was noted that HOXB7, which accumulates in membrane protrusions containing many peripheral actin structures, accumulated more in the S2-013 and PANC-1 cells cultured on fibronectin than in the corresponding cells not cultured on fibronectin (Fig. 1A). Z-stack panels showed that fibronectin-stimulated S2-013 cells exhibited intracellular expression of HOXB7 in the membrane protrusions (Fig. 1B).

Effects of HOXB7 knockdown on the cell motility and invasion of PDAC cells

To determine whether HOXB7 participates in the motility and invasiveness of PDAC cells, the expression of HOXB7 in S2-013 and PANC-1 cells was transiently suppressed by using *HOXB7*-specific siRNA oligonucleotides. Western blotting showed that 48 h after transfection, the expression of HOXB7 was markedly higher in control siRNA-transfected S2-013 and PANC-1 cells than in *HOXB7* siRNA-transfected cells (Fig. 2A). Consistent with the results of a previous report (10), the suppression of HOXB7 did not affect the growth of S2-013 or PANC-1 cells in an *in vitro* cell proliferation assay (data not shown). However, the suppression of HOXB7 inhibited the motility of S2-013 and PANC-1 cells in a transwell motility assay (Fig. 2B). Additionally, in a two-chamber Matrigel invasion assay, *HOXB7* siRNA-transfected S2-013 and PANC-1 cells were significantly less invasive than the control siRNA-transfected S2-013 and PANC-1 cells (Fig. 2C). When a HOXB7-rescue construct was transfected into *HOXB7* siRNA-transfected S2-013 and PANC-1 cells, exogenous HOXB7 localized to both the cytoplasm of cell bodies and to cell protrusions, similar to endogenous HOXB7 (Fig. 2, S2-013 cells (D) and S2-013 and PANC-1 cells (E)). Transfection of the HOXB7-rescue construct into *HOXB7* siRNA-transfected S2-013 and PANC-1 cells abrogated the changes in cell motility and invasiveness caused by the *HOXB7* siRNA (Fig. 2, B and C). These

results indicated that endogenous HOXB7 specifically promotes PDAC cell motility and invasion.

Roles of HOXB7 in the formation of cell protrusions

To determine whether HOXB7 is involved in the induction of membrane protrusion formation, we analyzed the peripheral actin structures in the membrane ruffles of fibronectin-stimulated control siRNA-transfected or *HOXB7* siRNA-transfected S2-013 and PANC-1 cells. Confocal microscopy showed that the HOXB7 that remained after HOXB7 knockdown in the *HOXB7* siRNA-transfected S2-013 and PANC-1 cells was localized to the cytoplasm of cell bodies and the nucleus and that *HOXB7* knockdown decreased the peripheral actin structures when compared with the corresponding control cells (Fig. 3, A and B). Furthermore, *HOXB7* knockdown significantly inhibited the fibronectin-stimulated formation of membrane protrusions when compared with the control S2-013 and PANC-1 cells (high magnification in Fig. 3 (C and D) and low magnification in supplemental Fig. S1 (A and B)).

Transfection of a HOXB7-rescue construct into *HOXB7* siRNA-transfected S2-013 and PANC-1 cells abrogated the decrease in peripheral actin structures in the membrane ruffles (high magnification in Fig. 4 (A and B) and low magnification in supplemental Fig. S2 (A and B)) and in the formation of cell protrusions (Fig. 4, C and D) that was caused by the *HOXB7* siRNA. Because the exogenous HOXB7 strongly accumulated in the cell protrusions of *HOXB7* siRNA-transfected S2-013 and PANC-1 cells (Fig. 4, E and F), HOXB7 localized to the cell protrusions could play a role in forming membrane protrusions in PDAC cells.

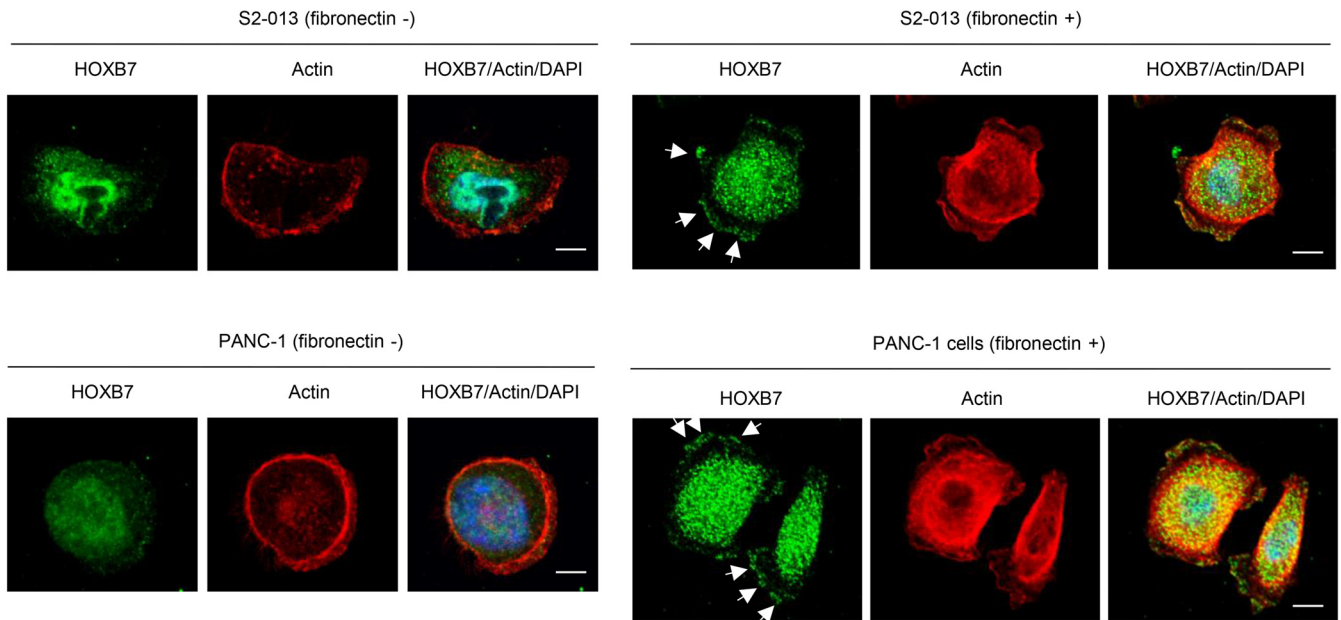
Association of HOXB7 with the regulation of Rho GTPase activation

Members of the Rho family, of which Rac1, Cdc42, and RhoA are the most commonly studied examples, play critical regulatory roles in several key cellular processes, such as the cytoskeletal rearrangement that underlies changes in cell shape, motility, and polarization (18, 19). To determine the effect of HOXB7 depletion on Rho GTPase activity, we assayed Rho GTPase activity in cell lysates by performing a GST pull-down assay using GST-p21-activated kinase-Cdc42/Rac interactive binding (CRIB) domain for Rac1 and Cdc42 and GST-rhotekin for RhoA. Suppression of HOXB7 with *HOXB7* siRNA oligonucleotides did not alter the levels of active Rac1 and Cdc42 when compared with the scrambled control siRNA-transfected S2-013 cells. In addition, suppression of HOXB7 with *HOXB7* siRNA oligonucleotides did not alter the levels of active RhoA (Fig. 5A).

Determination of protein phosphorylation patterns associated with HOXB7

We further analyzed intracellular signaling pathway molecules other than Rho GTPases in the scrambled control siRNA-transfected and *HOXB7* siRNA-transfected S2-013 cells cultured on fibronectin (Fig. 5B). We used a commercially available human phosphoprotein array kit that allowed semi-quantitative assessment of the levels of phosphorylated representatives of MAPKs, the Src family, and JAK/STAT pathways, among others. Of the 38 kinases studied, the suppression of HOXB7 resulted in the inactivation of ERK1/2 (Fig. 5, B and C);

A



B

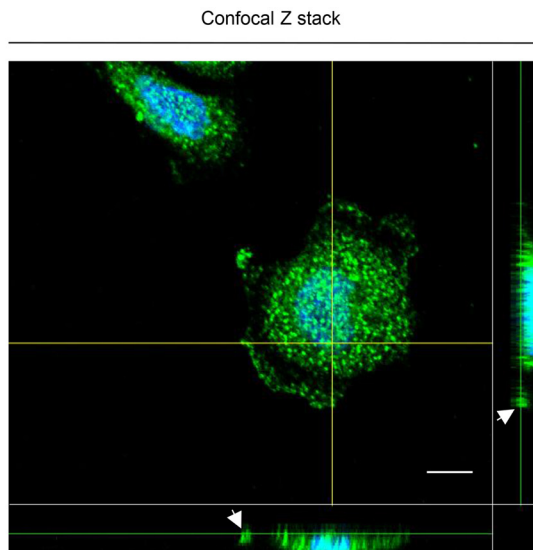


Figure 1. Subcellular localization of HOXB7 in PDAC cells. *A*, confocal immunofluorescence microscopy images. S2-013 and PANC-1 cells were cultured on fibronectin and then labeled with anti-HOXB7 antibody (green) and phalloidin (red). Actin filaments were labeled with phalloidin. Arrows, HOXB7 localized in cell protrusions. Blue, DAPI staining. Bars, 10 μ m. *B*, confocal Z stack shows nuclear DAPI staining (blue), abundant cytoplasmic HOXB7, and the accumulation of HOXB7 (green) in membrane protrusions of fibronectin-stimulated S2-013 cells. Actin filaments were labeled with phalloidin (red). Arrows, HOXB7 localized in cell protrusions. The bottom and right panels of the confocal Z stack show a vertical cross-section (yellow lines) through the cells. Bar, 10 μ m.

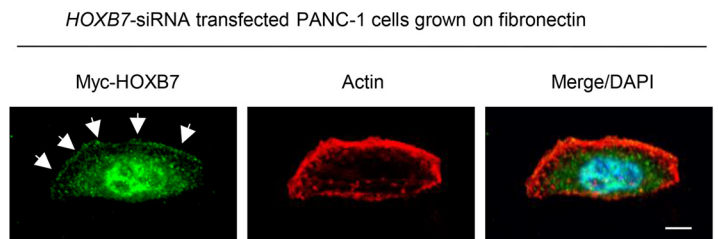
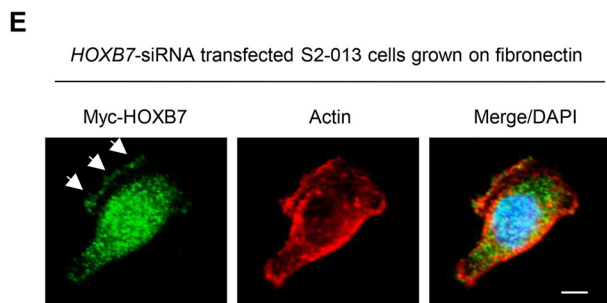
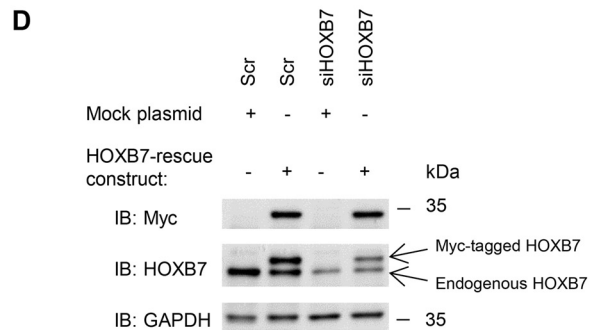
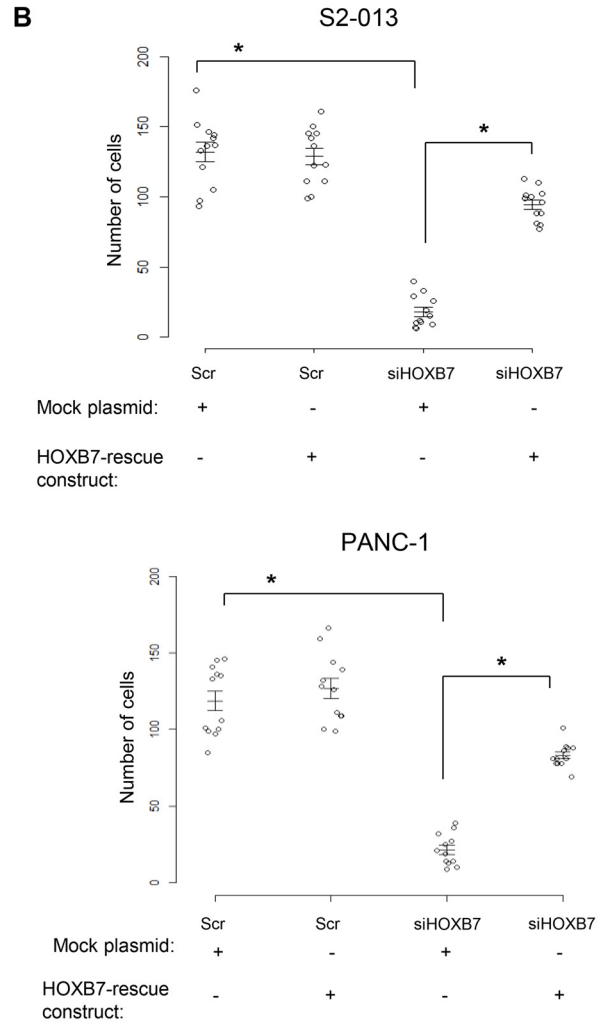
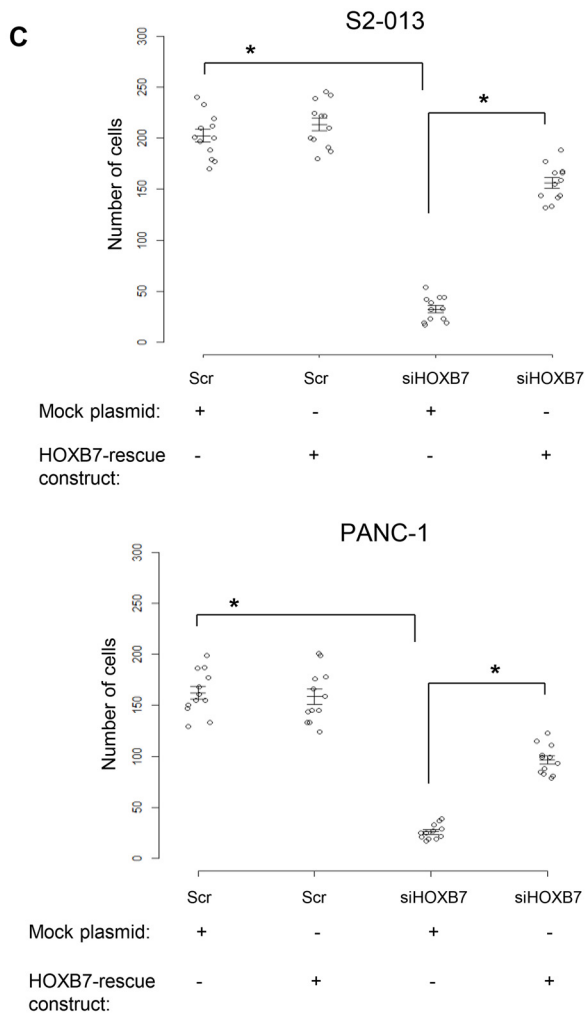
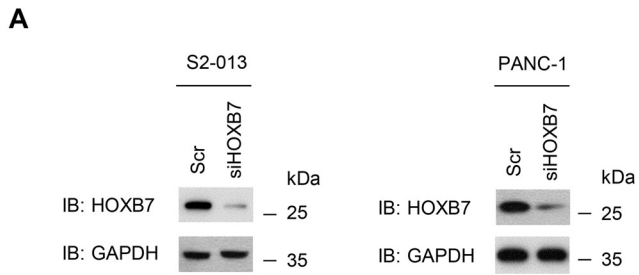
no change in phosphorylation of the other kinases, including Src family tyrosine kinases, was seen between the scrambled control siRNA-transfected S2-013 cells and the *HOXB7* siRNA-transfected S2-013 cells.

Association of HOXB7 and ERK1/2 with peripheral rearrangements of the actin cytoskeleton

In response to extracellular signals, Ras activates a kinase cascade that results in the phosphorylation of ERK1/2, which ultimately regulates the expression of genes involved in cell growth and survival (20). ERK signaling is not aberrantly up-

regulated in PDAC cells despite KRas proto-oncogene, GTPase (KRAS) expression, partly because of an increased expression of the MAPK phosphatase-2, which can inactivate ERK (21). To determine whether HOXB7 coordinates with ERK1/2 to promote peripheral rearrangements of the actin cytoskeleton, the subcellular distribution of phosphorylated ERK1/2 was examined in control siRNA-transfected or *HOXB7* siRNA-transfected S2-013 and PANC-1 cells cultured on fibronectin. Immunocytochemistry showed that phosphorylated ERK1/2 accumulated in the nucleus of the control S2-013 and PANC-1 cells, whereas little phosphorylated ERK1/2 was seen in the

HOXB7 promotes cell motility and invasion



nucleus of *HOXB7* siRNA-transfected S2-013 and PANC-1 cells (high magnification in Fig. 6A; low magnification in [supplemental Fig. S3A](#)). Suppression of *HOXB7* also decreased phosphorylated ERK1/2 localized to the cytoplasm of the cell bodies in S2-013 and PANC-1 cells (Fig. 6A). Transfection of the *HOXB7*-rescue construct into *HOXB7* siRNA-transfected S2-013 and PANC-1 cells abrogated the decrease in phosphorylated ERK1/2 in the nucleus and the cytoplasm (high magnification in Fig. 6B; low magnification in [supplemental Fig. S3B](#)). Subcellular fractionation of the cells showed that phosphorylated ERK1/2 levels were significantly lower in the nuclear and cytoplasmic fractions of *HOXB7* siRNA-transfected S2-013 and PANC-1 cells, compared with the levels in the control siRNA-transfected S2-013 and PANC-1 cells (Fig. 6, C and D). These results provide supportive evidence for the idea that *HOXB7* increased phosphorylated ERK1/2 in the nucleus and the cytoplasm of PDAC cells.

We next examined the actin cytoskeletal structures of scrambled control siRNA-transfected and *HOXB7* siRNA-transfected S2-013 and PANC-1 cells grown on fibronectin in the absence or presence of the MEK inhibitor U0126. In a previous study, inhibition of MEK activity by U0126 decreased the phosphorylation of its downstream kinase target ERK1/2, confirming inhibition of the MEK signaling pathway (22). In the present study, immunoblotting showed that U0126 decreased the phosphorylation of ERK1/2 in scrambled control siRNA-transfected S2-013 and PANC-1 cells grown on fibronectin (Fig. 7A). Another MEK-specific inhibitor, PD98059, is also known to decrease PDAC cell growth and ERK phosphorylation, although not as effectively as U0126 (22). ERK1/2 phosphorylation was partially blocked by the suppression of *HOXB7* (ranging from 40 to 60% inhibition) (Fig. 7A). Immunocytochemistry showed that treatment with 30 μM U0126 decreased the level of phosphorylated ERK1/2 in the nucleus and the cytoplasm and inhibited surface actin rearrangement (Fig. 7B) and the formation of cell protrusions (Fig. 7C) in scrambled control siRNA-transfected S2-013 and PANC-1 cells, similar to non-treated *HOXB7* siRNA-transfected S2-013 and PANC-1 cells. These results indicated that *HOXB7* plays a role in promoting peripheral actin cytoskeletal rearrangement by increasing the levels of phosphorylated ERK1/2 in the nucleus and the cytoplasm.

Association of *HOXB7* and ERK1/2 with the cell motility and invasiveness of PDAC cells

To evaluate the effects of U0126 on the cell motility and invasiveness of PDAC cells, we carried out *in vitro* motility and

invasion assays. Pretreatment of scrambled control siRNA-transfected S2-013 and PANC-1 cells with U0126 significantly inhibited cell motility and invasion (Fig. 8, A and B). Importantly, U0126 decreased the cell motility and invasiveness of the scrambled control S2-013 and PANC-1 cells to the same levels as those of the *HOXB7* siRNA-transfected S2-013 and PANC-1 cells that had not been pretreated with U0126. These results indicated that activated ERK1/2 plays an important role in accelerating cell motility and invasion and that the *HOXB7*-dependent promotion of PDAC cell motility and invasion is probably associated with an increase in active ERK1/2.

The association of *HOXB7* and ERK1/2 with cell motility and invasion was evaluated. Transfection of the *HOXB7*-rescue construct into *HOXB7* siRNA-transfected S2-013 and PANC-1 cells treated with U0126 had no effect on cell motility or invasiveness when compared with the corresponding mock-transfected U0126-treated cells (Fig. 8, C and D). These results indicated that *HOXB7* plays a role in promoting cell motility and invasion by increasing the levels of phosphorylated ERK1/2.

Association of *HOXB7* with ERK1/2 regulates the expression of motility and invasiveness-related genes

To identify genes whose functions are associated with *HOXB7* and ERK1/2 in PDAC cells, global gene expression profiling was performed in *HOXB7* siRNA-transfected S2-013 cells that were transfected with a *HOXB7*-rescue construct and subsequently incubated on fibronectin with or without U0126. The microarray data have been deposited with the NCBI Gene Expression Omnibus (GEO) under the accession number GSE97969. Hierarchical cluster analysis identified that U0126 treatment up-regulated 71 genes and down-regulated 97 genes whose expression was significantly altered ($-\text{fold change } e \geq 2.0$) when compared with non-treated cells (Fig. 9A and [supplemental Tables S1 and S2](#)). Gene ontology (GO) analysis showed that the most highly enriched GO terms for these genes included “cell migration,” “cell motility,” “localization of cell,” “regulation of cell adhesion,” and “extracellular matrix organization” (Fig. 9B).

This global gene expression profiling showed decreased expression of five MAPK-associated genes in *HOXB7* siRNA-transfected S2-013 cells transfected with a *HOXB7*-rescue construct and subsequently incubated on fibronectin with U0126 as compared with identical cells subsequently incubated on fibronectin without U0126 ($-\text{fold change } \geq 1.5$; Fig. 9C). We focused on the HRas proto-oncogene, GTPase (HRAS). Active RAS stimulates mitogenic and survival signal transduction by

Figure 2. Roles of *HOXB7* in cell motility and invasion. A, Western blotting (IB) with anti-*HOXB7* antibody. A single mixture with four different siRNA oligonucleotides targeting *HOXB7* (*siHOXB7*) or a single mixture with four different scrambled control siRNA oligonucleotides (*Scr*) was transiently transfected into S2-013 and PANC-1 cells. Western blotting was performed using anti-*HOXB7* antibody. B, transwell motility assay. Oligonucleotides (siRNAs targeting *HOXB7* (*siHOXB7*), or scrambled siRNAs (*Scr*) as the negative control) were transiently transfected into S2-013 and PANC-1 cells. Subsequently, a mock control vector or a Myc-tagged *HOXB7*-rescue construct was transiently transfected into *HOXB7* siRNA-transfected S2-013 and PANC-1 cells; 48 h later, a transwell motility assay was performed. Migrating cells in four visual fields per group were scored. Data are derived from three independent experiments. Columns, mean; bars, S.E. *, $p < 0.02$ (Student's *t* test). C, Matrigel invasion assay. Scrambled control siRNA-transfected S2-013 and PANC-1 cells and *HOXB7* siRNA-transfected S2-013 and PANC-1 cells were seeded into Matrigel invasion chambers. Subsequently, a mock control vector or a Myc-tagged *HOXB7*-rescue construct was transiently transfected into *HOXB7* siRNA-transfected S2-013 and PANC-1 cells; 48 h later, a Matrigel invasion assay was performed. Invading cells in four visual fields per group were counted. Data are derived from three independent experiments. Columns, mean; bars, S.E. *, $p < 0.02$ (Student's *t* test). D, a mock control vector or a Myc-tagged *HOXB7*-rescue construct was transiently transfected into scrambled control siRNA-transfected S2-013 cells and *HOXB7* siRNA-transfected S2-013 cells. Western blotting was performed using anti-Myc and anti-*HOXB7* antibodies. E, confocal immunofluorescence microscopy images. A Myc-tagged *HOXB7*-rescue construct was transfected into *HOXB7* siRNA-transfected S2-013 and PANC-1 cells; 48 h later, the cells were incubated on fibronectin. The cells were then stained with anti-Myc antibody (green). Actin filaments were labeled with phalloidin (red). Blue, DAPI staining. Bars, 10 μm .

HOXB7 promotes cell motility and invasion

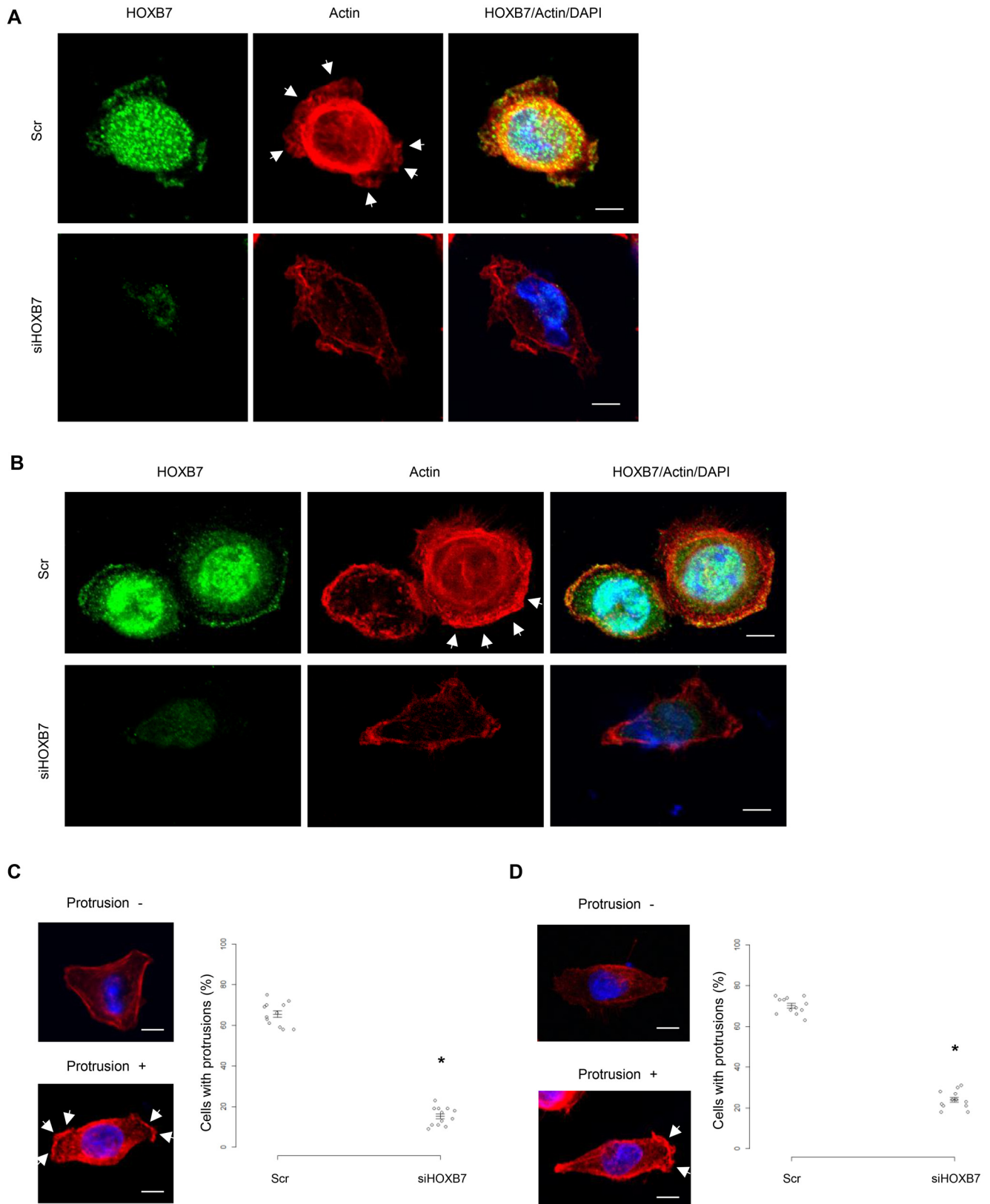
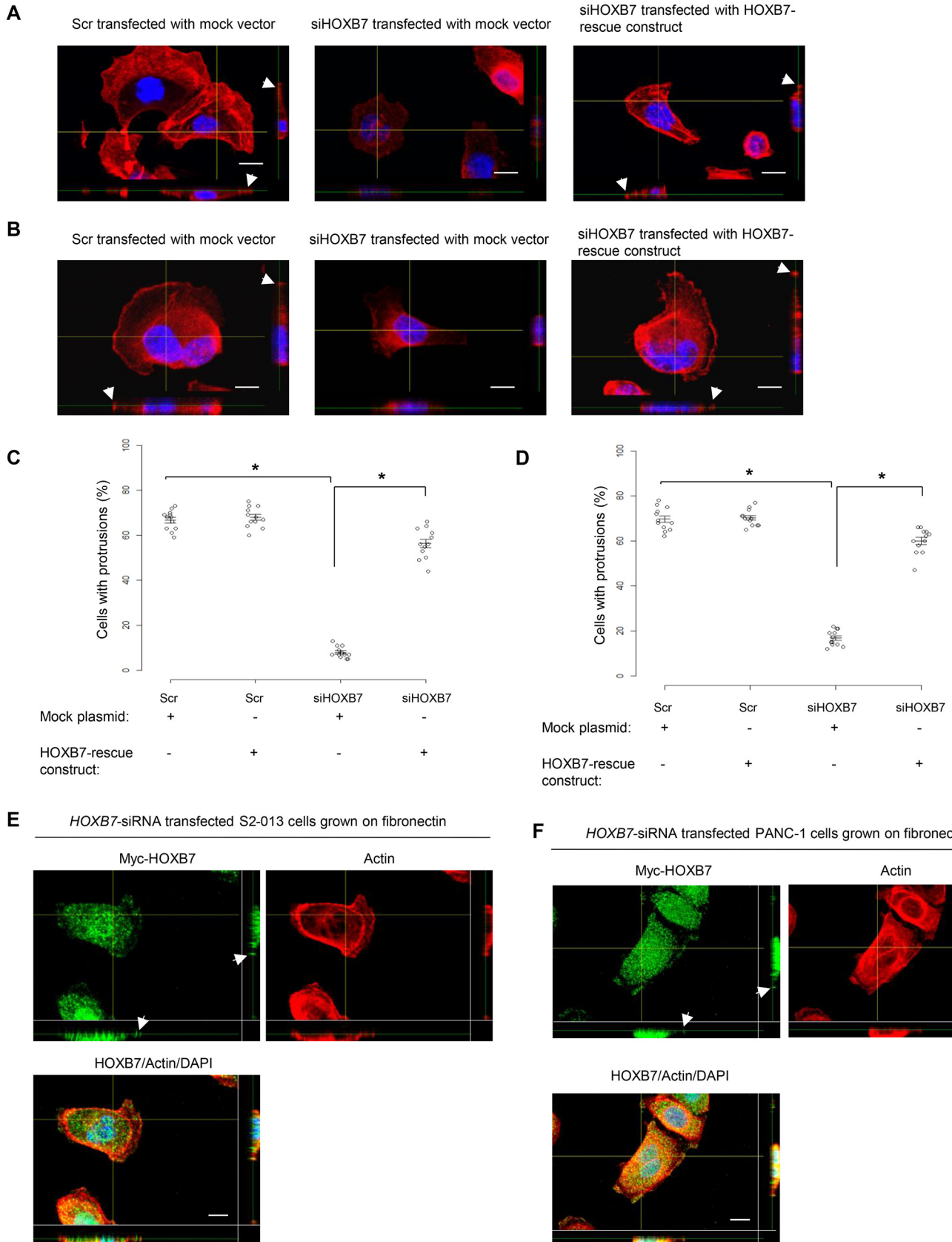
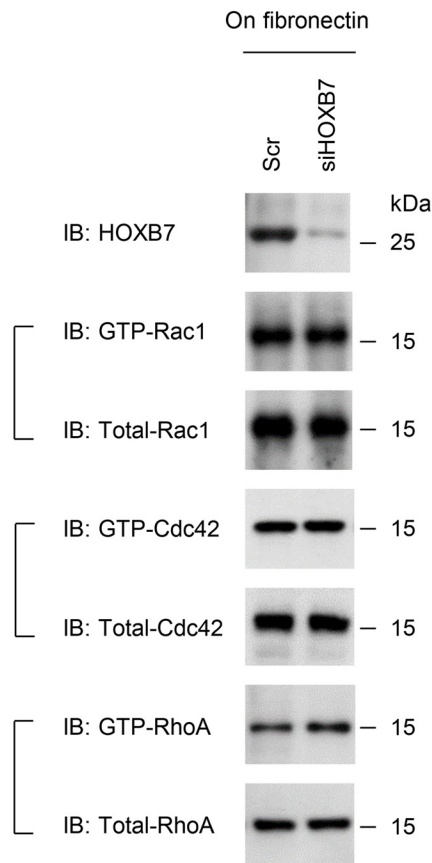


Figure 3. Effects of the suppression of HOXB7 on the formation of cell protrusions. *A* and *B*, confocal immunofluorescence microscopy images. Oligonucleotides (siRNAs targeting *HOXB7* (siHOXB7) or scrambled RNAs (Scr) as the negative control) were transiently transfected into S2-013 (*A*) and PANC-1 (*B*) cells. The transfected cells were incubated on fibronectin and subsequently stained with anti-HOXB7 antibody (green) and phalloidin (red). Arrows, peripheral actin structures in cell protrusions of scrambled RNA-transfected cells. Blue, DAPI staining. Bars, 10 μ m. *C* and *D*, quantification of the data shown in *A* (*C*) and *B* (*D*). Four independent visual fields were examined via microscopic observation to count the number of cells that formed cell protrusions. Data are derived from three independent experiments. Arrows, peripheral actin structures in cell protrusions. Columns, mean; bars, S.E. *, $p < 0.001$ compared with scrambled RNA-transfected controls (Student's *t* test). Bars, 10 μ m.

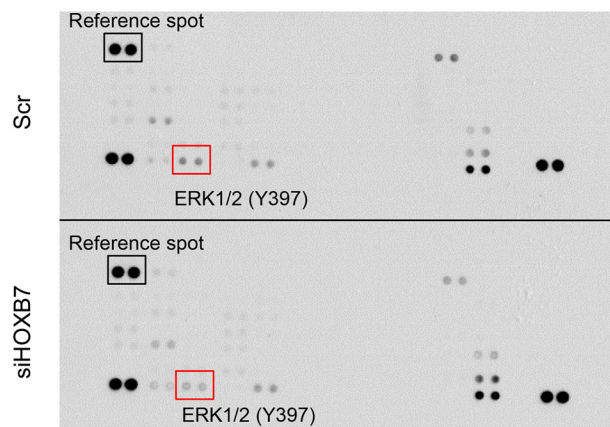


HOXB7 promotes cell motility and invasion

A



B



C

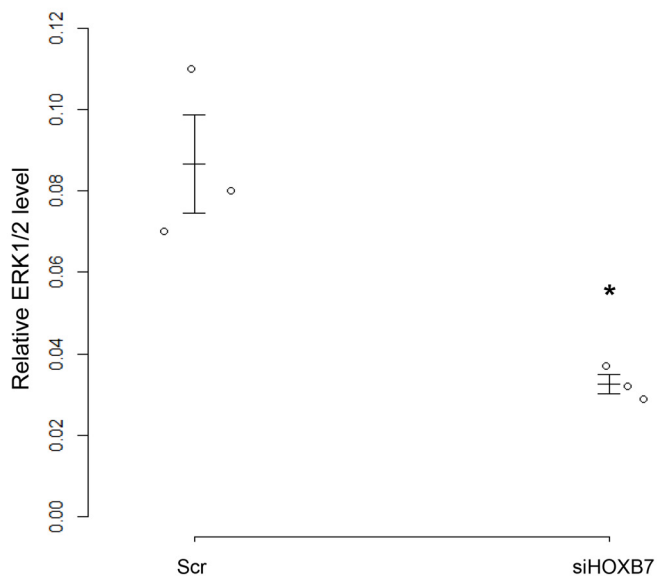
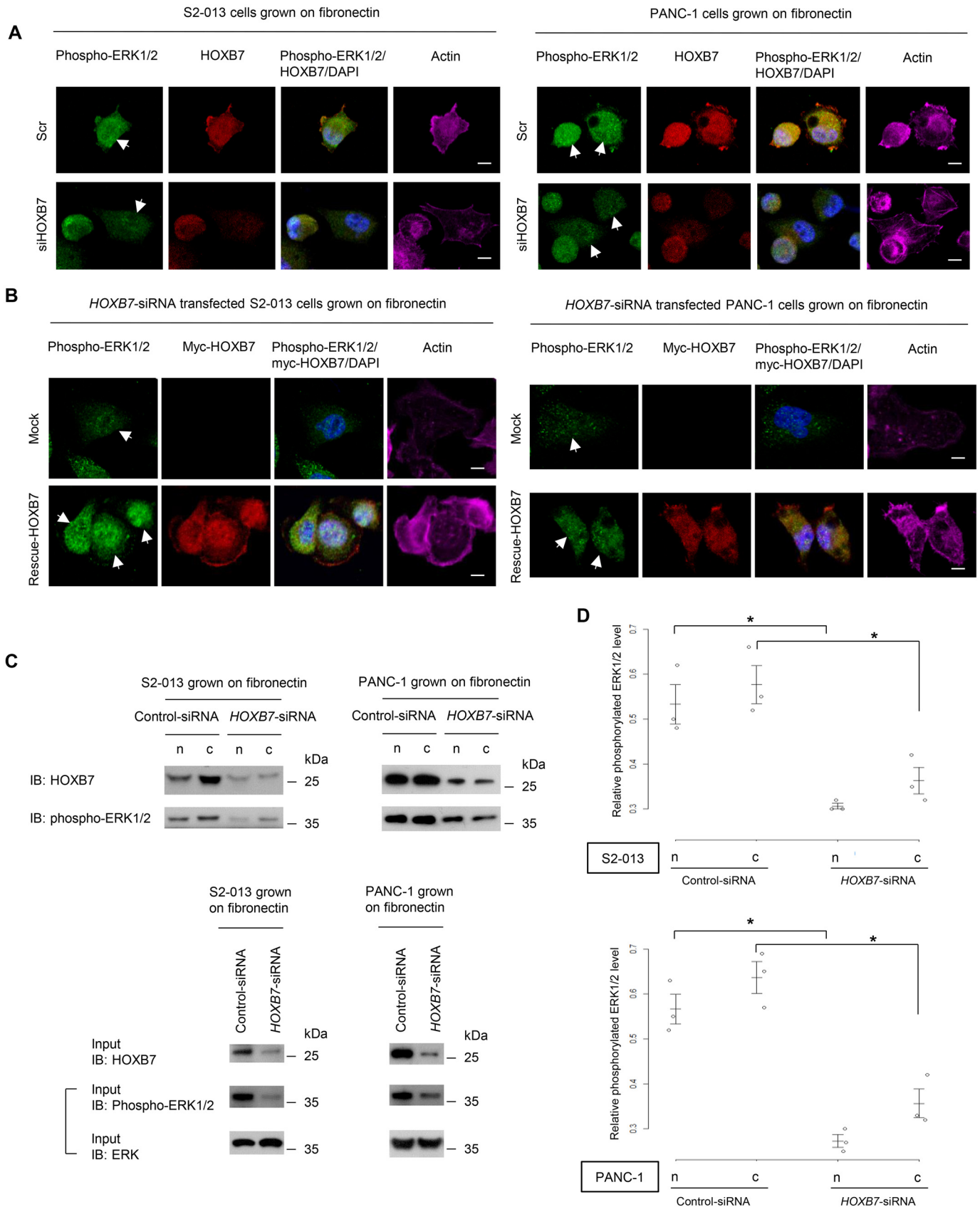


Figure 5. Roles of HOXB7 in the regulation of Rho GTPase activation and determination of protein phosphorylation patterns associated with HOXB7. *A*, GST pull-down assays of active Rho GTPases in scrambled control siRNA-transfected S2-013 and *HOXB7* siRNA-transfected S2-013 cells. Scrambled control siRNA (*Scr*) or *HOXB7* siRNA (*siHOXB7*) oligonucleotides were transfected into S2-013 cells; 48 h later, the cells were incubated on fibronectin for 5 h, and the amounts of active GTP-loaded Rac1, Cdc42, and RhoA were determined using GST pull-down assays. Precipitates were examined by Western blotting (*IB*) using anti-HOXB7, anti-Rac1, anti-Cdc42, and anti-RhoA antibodies. Data are representative of three independent experiments. *B*, effects of the suppression of HOXB7 on the expression of selected phosphoproteins in S2-013 cells. Cell extracts obtained from scrambled control siRNA-transfected S2-013 cells or *HOXB7* siRNA-transfected S2-013 cells grown on fibronectin were probed using human phosphoprotein arrays. Data are representative of three independent experiments. *C*, densitometric analysis of the results of *B*. The levels of phosphorylated ERK1/2 in *HOXB7* siRNA-transfected S2-013 cells were compared with those in scrambled control siRNA-transfected S2-013 cells. The levels of phosphorylated ERK1/2 were assessed after normalizing phosphorylated ERK1/2 signals to the reference spot signals. Data are derived from three independent experiments. *Columns*, mean; *bars*, S.E. *, $p < 0.02$ compared with scrambled control siRNA-transfected S2-013 cells (Student's *t* test).

Figure 4. Effects of transfection of the HOXB7-rescue construct into HOXB7 siRNA-transfected PDAC cells on the formation of cell protrusions. *A* and *B*, confocal Z-stack immunofluorescence microscopy images showing phalloidin-labeled peripheral actin structures (*red*) and DAPI-labeled nuclei (*blue*) in scrambled control siRNA-transfected S2-013 and PANC-1 cells (*Scr*) or *HOXB7* siRNA-transfected S2-013 and PANC-1 cells (*siHOXB7*) transfected with or without a Myc-tagged HOXB7-rescue construct. The transfected cells were incubated on fibronectin and subsequently stained. S2-013 and PANC-1 cells are shown in *A* and *B*, respectively. *Arrows*, peripheral actin structures in cell protrusions. The *bottom* and *right panels* of the confocal Z stack show a vertical cross-section (*yellow lines*) through the cells. *Bars*, 10 μm . *C* and *D*, quantification of the data shown in *A* (*C*) and *B* (*D*); the values represent the number of cells with fibronectin-stimulated cell protrusions in which peripheral actin structures increased. All cells in four visual fields per group were scored. Data are derived from three independent experiments. *Columns*, mean; *bars*, S.E. *, $p < 0.001$ (Student's *t* test). *E* and *F*, confocal Z-stack immunofluorescence microscopy images of HOXB7 cellular localization in *HOXB7* siRNA-transfected S2-013 and PANC-1 cells that were subsequently transfected with a Myc-tagged HOXB7-rescue construct; 48 h later, the cells were incubated on fibronectin. The cells were stained with anti-Myc antibody (*green*). Actin filaments were labeled with phalloidin (*red*). S2-013 and PANC-1 cells are shown in *E* and *F*, respectively. *Arrows*, exogenous HOXB7 accumulated in cell protrusions. The *bottom* and *right panels* of the confocal Z stack show a vertical cross-section (*yellow lines*) through the cells. *Bars*, 10 μm .



HOXB7 promotes cell motility and invasion

coupling to effectors, including rapidly accelerated fibrosarcoma (RAF) kinase for propagation of the MAPK pathway (RAS/RAF/MEK/ERK) and PI3K pathways (23). The HRAS expression level was decreased in U0126-treated *HOXB7* siRNA-transfected S2-013 cells that were transfected with a *HOXB7*-rescue construct, compared with non-treated identical cells (Fig. 9, *D* and *E*). Treatment with U0126 did not decrease the expression levels of another RAS isoform KRAS and NRAS proto-oncogene, GTPase (NRAS) (Fig. 9, *D* and *E*).

The mechanisms by which HOXB7 exerts its effects on ERK1/2 activity

We analyzed intracellular signaling pathway molecules associated with *HOXB7* and ERK1/2 in *HOXB7* siRNA-transfected S2-013 cells that were transfected with a *HOXB7*-rescue construct and subsequently incubated on fibronectin with or without U0126 by using a human phosphoprotein array kit. This array showed that treatment with U0126 decreased ERK1/2 activity (Fig. 10A). Of the 38 kinase phosphorylation sites studied, treatment with U0126 resulted in the dephosphorylation of JNK and HSP27 (Fig. 10, *A* and *B*). Immunoblotting confirmed that treatment of *HOXB7* siRNA-transfected S2-013 cells that were transfected with the *HOXB7*-rescue construct with U0126 decreased the phosphorylation levels of ERK1/2, JNK, and HSP27, compared with the non-treated cells (Fig. 10C).

To determine whether *HOXB7* altered the phosphorylation levels of JNK and HSP27, immunoblotting was performed in the control siRNA-transfected and *HOXB7* siRNA-transfected S2-013 cells cultured on fibronectin (Fig. 10D). Because the signal intensities of phosphorylated JNK and HSP27 were not obvious in the phosphoprotein array shown in Fig. 5B, we confirmed that suppression of *HOXB7* decreased the phosphorylation levels of JNK and HSP27 (Fig. 10D).

Up-regulated expression of HRAS increased HOXB7-associated ERK1/2 activity, motility, and invasiveness

Immunoblotting showed that, 48 h after transfection with *HRAS*-specific or control siRNAs into S2-013 cells, the expression of *HRAS* was markedly higher, but *KRAS* and *NRAS* expression levels were unchanged in the control siRNA-transfected S2-013 cells (Fig. 11A). It is notable that suppression of *HRAS* decreased the phosphorylation levels of ERK1/2, JNK, and HSP27, but phosphorylated Akt, a kinase implicated in the PI3K signaling pathway (23), was unchanged (Fig. 11A).

Transfection of a *HOXB7*-rescue construct into S2-013 cells in which both *HOXB7* and *HRAS* were suppressed by the use of *HOXB7* siRNAs and *HRAS* siRNAs did not increase the phosphorylation levels of ERK1/2, JNK, and HSP27, whereas

transfection of a *HOXB7*-rescue construct into *HOXB7* siRNA-transfected S2-013 cells did increase the phosphorylation levels of ERK1/2, JNK, and HSP27, to nearly the same levels as in scrambled control siRNA-transfected S2-013 cells that were not transfected with *HRAS* siRNAs (Fig. 11B). The levels of phosphorylated Akt were unchanged in these cells (Fig. 11B). Together with the findings shown in Figs. 7A and 10C, these results indicated that *HRAS* was necessary for regulation of the phosphorylation levels of ERK1/2, JNK, and HSP27 through *HOXB7*.

In transwell motility assays, the motility of S2-013 cells was significantly lower in *HRAS*-knockdown cells than in control cells (Fig. 11C). In two-chamber invasion assays, the invasiveness of S2-013 cells was significantly lower in *HRAS*-knockdown cells than in control cells (Fig. 11C). Transfection of a *HOXB7*-rescue construct into S2-013 cells in which both *HOXB7* and *HRAS* had been suppressed did not abrogate the changes to cell motility and invasiveness caused by the *HOXB7* siRNAs and *HRAS* siRNAs (Fig. 11D). These results indicated that, at least in part, *HRAS* was necessary for the *HOXB7*-associated promotion of motility and invasiveness.

Association of JNK and HSP27 with peripheral rearrangements of the actin cytoskeleton

Immunoblotting showed that JNK phosphorylation in S2-013 cells was blocked by the JNK inhibitor SP600125 at a dose of 20 μM (Fig. 12A) and that 48 h after transfection with *HSP27*-specific or control siRNAs into S2-013 cells, the expression of *HSP27* was markedly higher in the control siRNA-transfected S2-013 cells (Fig. 12B). Active JNK is localized in the cytoplasm as well as in the nucleus (24). Active *HSP27* is localized in the entire cytoplasm of the cells and in the cell periphery (25). Immunocytochemistry showed that treatment with SP600125 decreased the level of phosphorylated JNK in the nucleus and the cytoplasm and inhibited surface actin rearrangement in S2-013 cells grown on fibronectin (Fig. 12C). *HSP27* knockdown also decreased the peripheral actin structures, compared with control siRNA-transfected S2-013 cells (Fig. 12D). Treatment with SP600125 and *HSP27* knockdown inhibited the formation of cell protrusions in S2-013 cells grown on fibronectin (Fig. 12, *E* and *F*). These results indicated that JNK and *HSP27* play important roles in promoting peripheral actin cytoskeletal rearrangements and the formation of cell protrusions.

Association of HOXB7 with JNK and HSP27 in regulation of the motility and invasiveness of PDAC cells

To evaluate whether JNK and *HSP27* are necessary for *HOXB7* to promote cell motility and invasion, we performed

Figure 6. Association of HOXB7 and phosphorylated ERK1/2 with peripheral rearrangements of the actin cytoskeleton. *A*, confocal immunofluorescence microscopy images. Oligonucleotides (siRNAs targeting *HOXB7* (*siHOXB7*), or scrambled RNAs (*Scr*) as the negative control) were transiently transfected into S2-013 and PANC-1 cells. The transfected cells were incubated on fibronectin and subsequently stained with anti-phosphorylated ERK1/2 antibody (green), anti-*HOXB7* antibody (red), and phalloidin (violet). Arrows, phosphorylated ERK1/2 in the nucleus. Blue, DAPI staining. Bars, 10 μm . *B*, confocal immunofluorescence microscopy images. A Myc-tagged *HOXB7*-rescue construct was transfected into *HOXB7* siRNA-transfected S2-013 and PANC-1 cells; 48 h later, the cells were incubated on fibronectin. The cells were stained with anti-phosphorylated ERK1/2 antibody (green), anti-Myc antibody (red), and phalloidin (violet). Arrows, phosphorylated ERK1/2 in the nucleus. Blue, DAPI staining. Bar, 10 μm . *C*, scrambled RNA-transfected S2-013 and PANC-1 cells and *siHOXB7*-transfected S2-013 and PANC-1 cells were incubated on fibronectin and fractionated into cytosolic (*c*) and nuclear (*n*) fractions. Western blotting (*IB*) of the fractions was performed using anti-*HOXB7*, anti-phosphorylated ERK1/2, and anti-ERK1/2 antibodies. *D*, densitometric analysis of the results of Fig. 6C. The levels of phosphorylated ERK1/2 localized in each fraction were assessed after normalizing phosphorylated ERK1/2 signals to input samples. Data are derived from three independent experiments. Columns, mean; bars, S.E. *, $p < 0.02$ compared with the corresponding scrambled control siRNA-transfected cells (Student's *t* test).

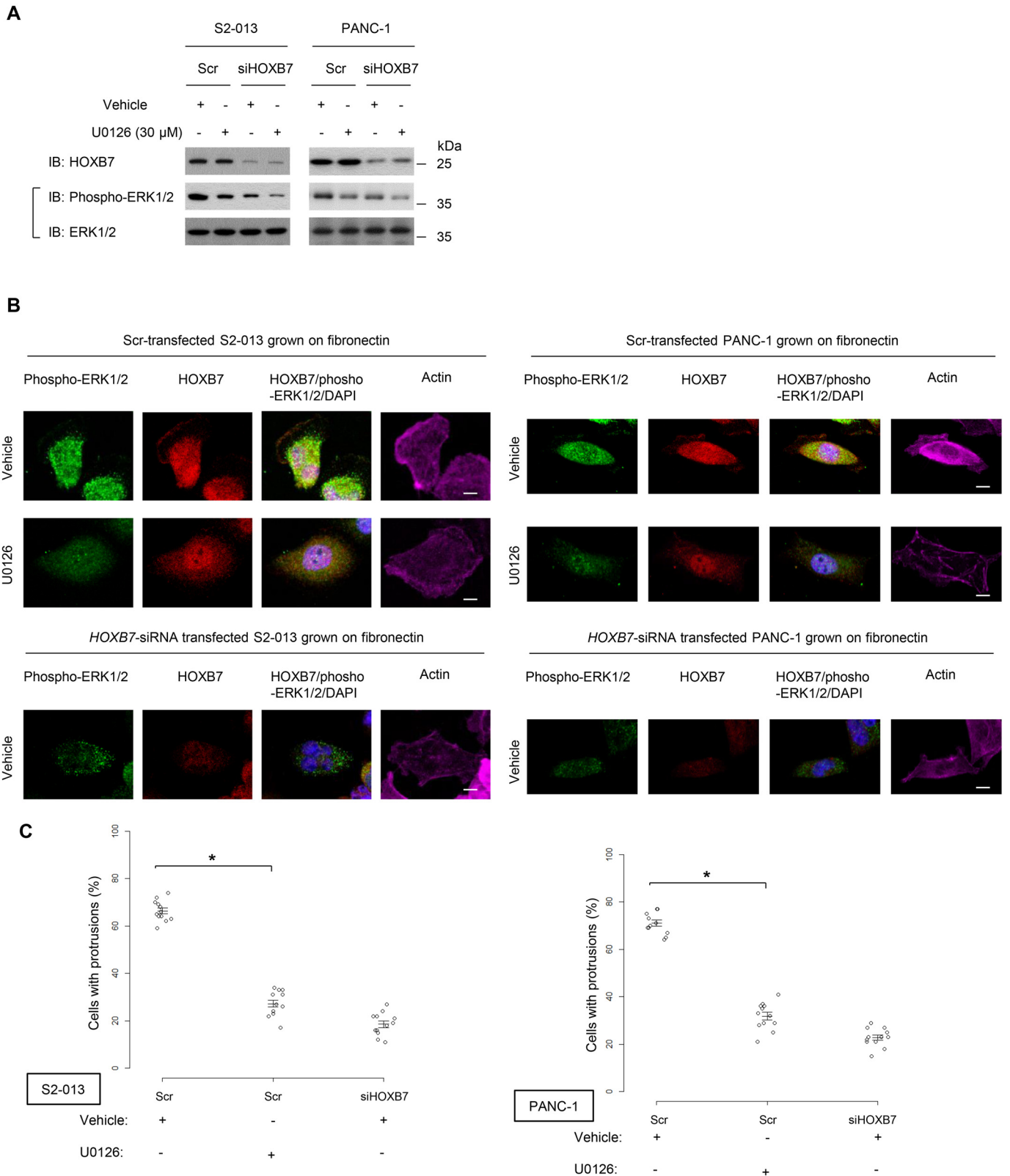


Figure 7. Effects of a MEK inhibitor and knockdown of HOXB7 on the formation of cell protrusions. *A*, scrambled control-siRNA-transfected (*Scr*) S2-013 and PANC-1 cells and *HOXB7*-siRNA-transfected (*siHOXB7*) S2-013 and PANC-1 cells incubated on fibronectin were treated with a MEK inhibitor (30 μ M U0126) or with vehicle only. The cells were lysed, and equivalent amounts of whole tissue lysates were subjected to Western blotting (*IB*) with the indicated antibodies. *B*, confocal immunofluorescence microscopy images. S2-013 and PANC-1 cells were treated as described in *A*. *HOXB7* siRNA-transfected cells were treated with vehicle only. Cells were stained with anti-phosphorylated ERK1/2 antibody (*green*), anti-*HOXB7* antibody (*red*), and phalloidin (*violet*). *Blue*, DAPI staining. *Bars*, 10 μ m. *C*, quantification of the data shown in *B*. Four independent visual fields were examined via microscopic observation to count the number of cells that formed cell protrusions. Data are derived from three independent experiments. *Columns*, mean; *bars*, S.E. *, $p < 0.001$ compared with the corresponding controls (Student's *t* test).

HOXB7 promotes cell motility and invasion

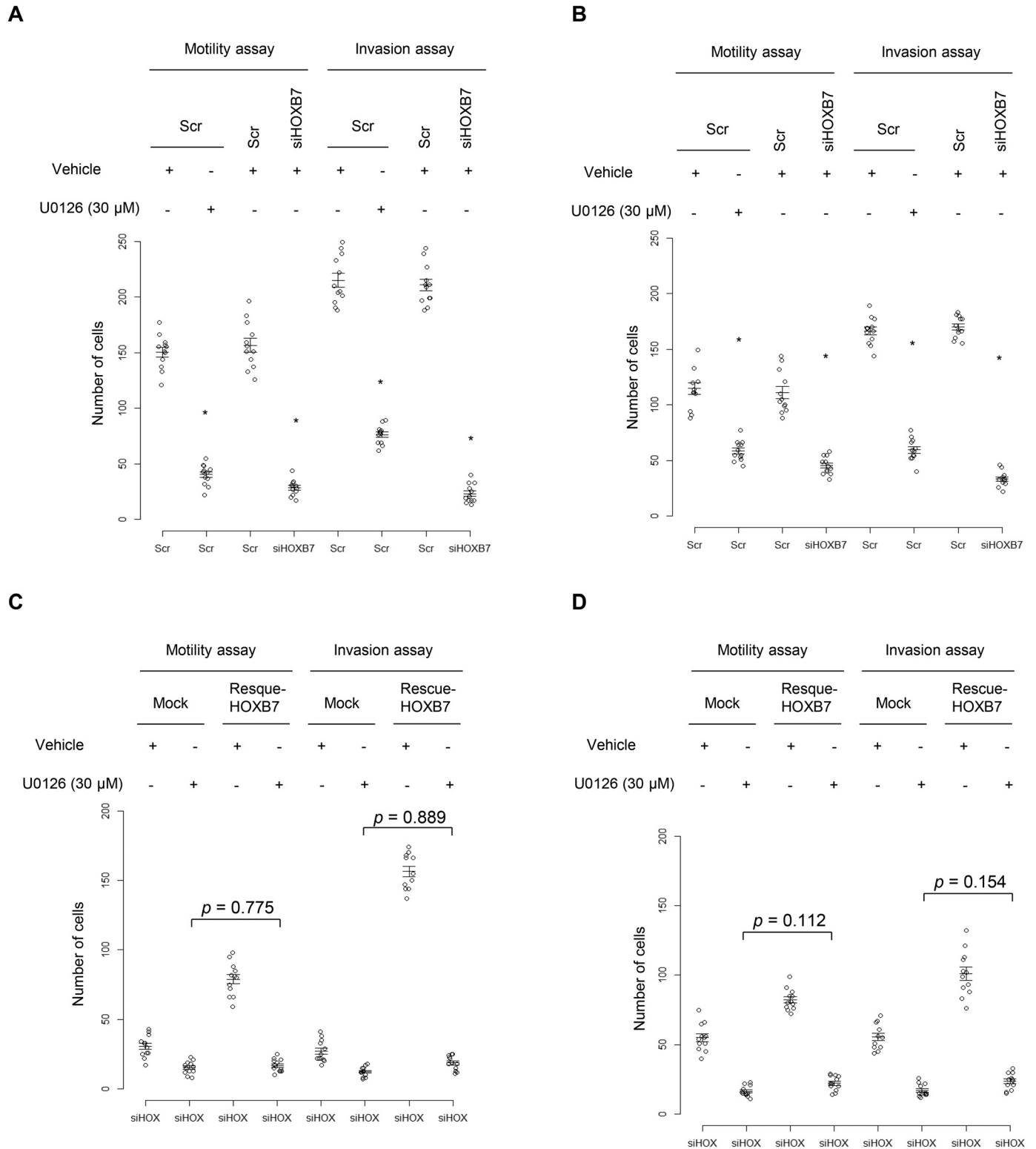


Figure 8. Association of HOXB7 and ERK1/2 with cell motility and invasiveness. A and B, a transwell motility assay and a Matrigel invasion assay were performed using S2-013 (A) and PANC-1 (B) cells treated as described in A (30 μ M U0126). Migrating cells in four visual fields per group were scored. Data are derived from three independent experiments. Columns, mean; bars, S.E. *, $p < 0.02$ compared with the corresponding scrambled RNA (Scr)-transfected controls (Student's t test). C and D, transwell motility assay and Matrigel invasion assay. A Myc-tagged HOXB7-rescue construct was transfected into S2-013 (C) and PANC-1 (D) cells that had been transfected with HOXB7 siRNA; 48 h later, the cells were incubated on fibronectin with or without U0126 and were subsequently used for a transwell motility assay and a Matrigel invasion assay. Migrating cells in four visual fields per group were scored. Data are derived from three independent experiments. Columns, mean; bars, S.E.

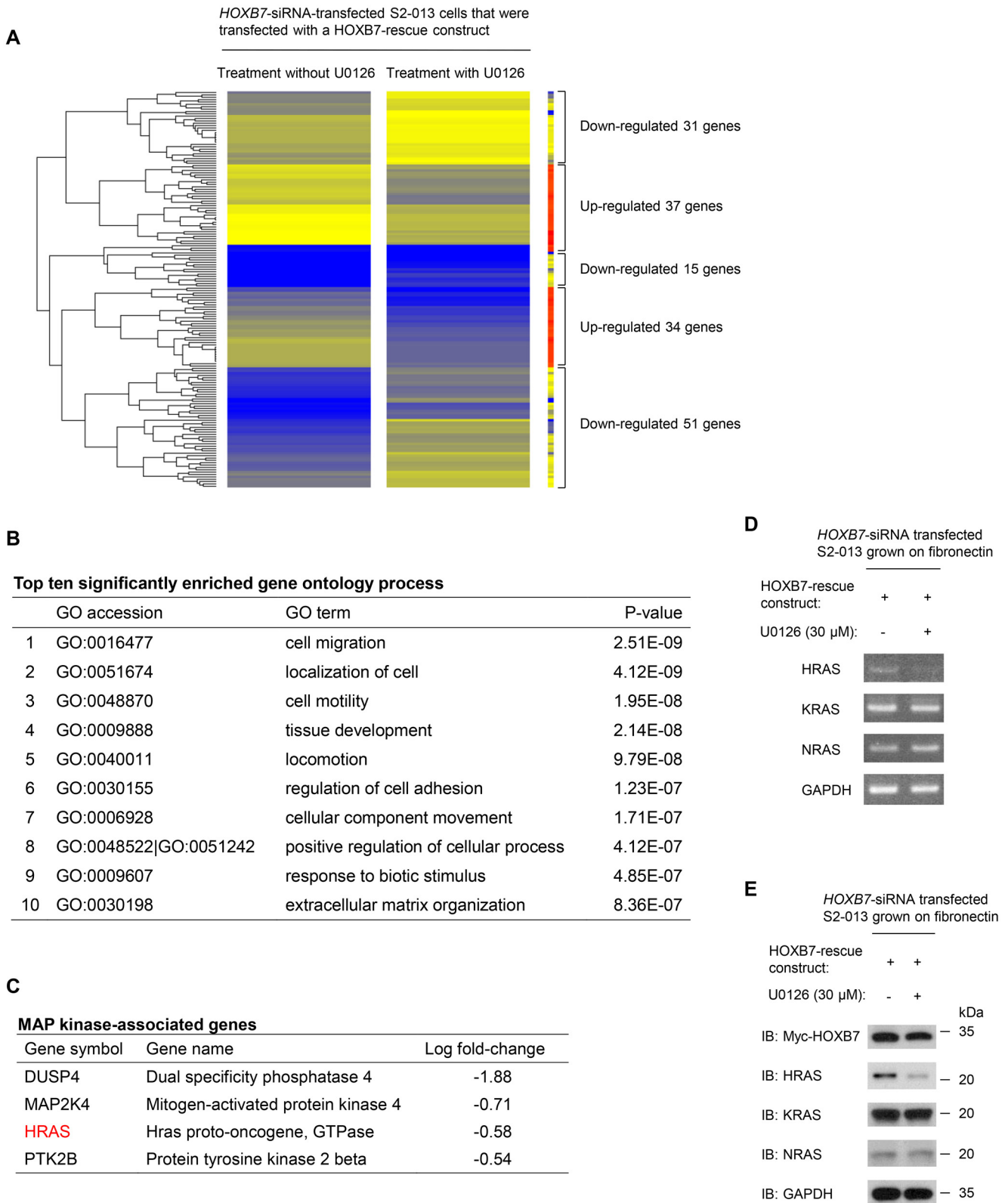


Figure 9. Expression profiling shows that *HOXB7* and ERK1/2 regulate the expression of motility and invasion-related genes. *A*, gene expression profiling was carried out in *HOXB7* siRNA-transfected S2-013 cells that were transfected with a *HOXB7*-rescue construct and subsequently incubated on fibronectin with or without U0126. Shown are significant differentially expressed genes at $p < 0.05$ corrected for false discovery rate, together with -fold change ≥ 2.0 . *B*, GO category enrichments of the genes differentially regulated by U0126 treatment of *HOXB7* siRNA-transfected S2-013 cells that were transfected with a *HOXB7*-rescue construct. *C*, MAPK signaling pathway genes down-regulated by U0126 treatment of *HOXB7* siRNA-transfected S2-013 cells that were transfected with a *HOXB7*-rescue construct. *D* and *E*, RT-PCR analysis (*D*) and Western blotting (*IB*) (*E*) of the steady-state levels of HRAS, KRAS, and NRAS in *HOXB7* siRNA-transfected S2-013 cells that were transfected with a *HOXB7*-rescue construct and subsequently incubated on fibronectin with or without U0126.

HOXB7 promotes cell motility and invasion

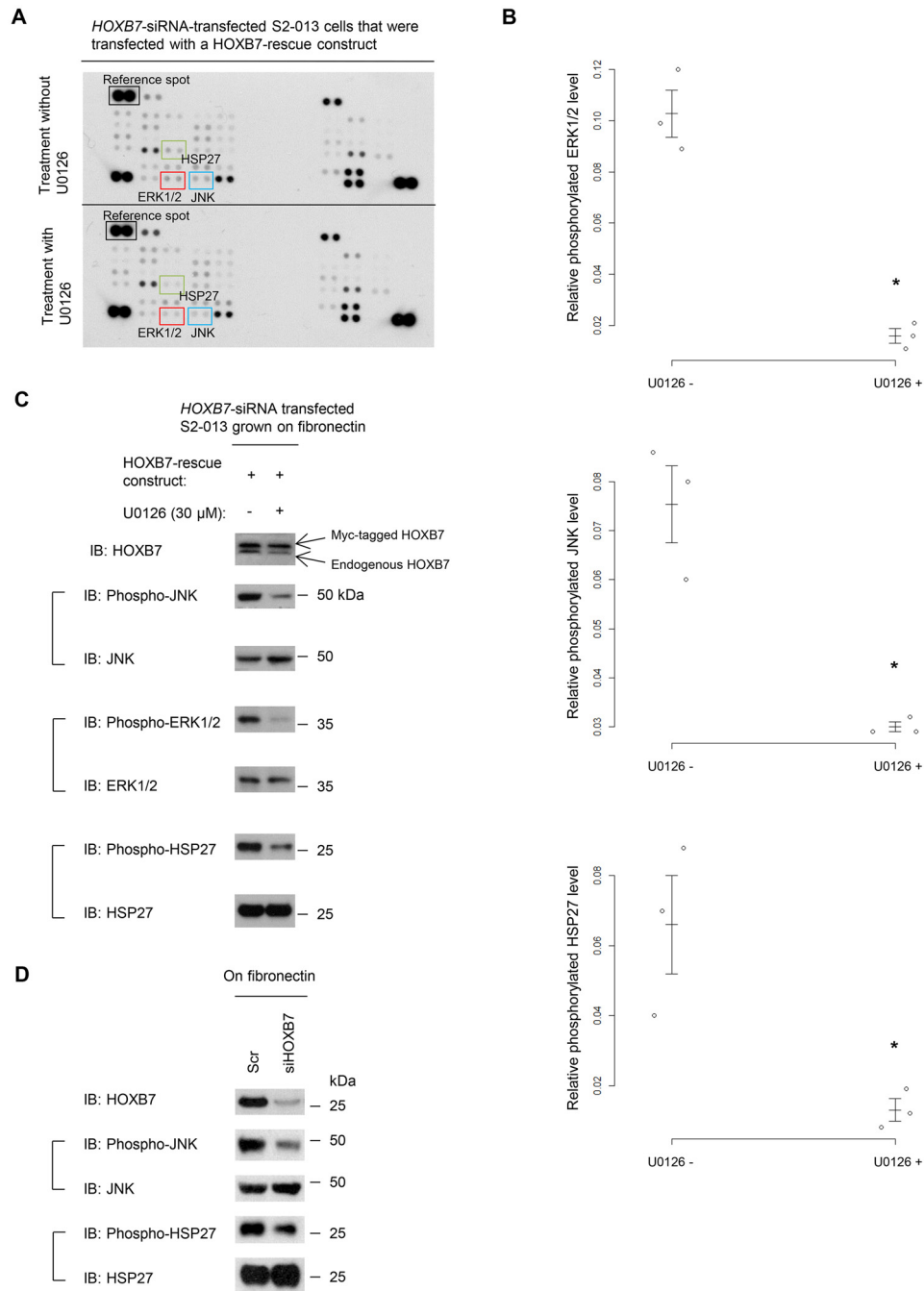


Figure 10. Signaling pathway molecules associated with HOXB7 and ERK1/2. A, a HOXB7-rescue construct was transfected into S2-013 cells that had been transfected with *HOXB7* siRNA; 48 h later, the cells were incubated on fibronectin with or without U0126. Cell extracts were probed using human phospho-protein arrays. B, densitometric analysis of the results of A. The levels of phosphorylated JNK and phosphorylated HSP27 in cells treated with U0126 were compared with those in the non-treated cells. Data are derived from three independent experiments. Columns, mean; bars, S.E. *, $p < 0.05$ compared with the non-treated cells (Student's *t* test). C, S2-013 cells treated as described in A were lysed, and equivalent amounts of whole-cell lysates were subjected to Western blotting (IB) with the indicated antibodies. D, a single mixture with four different siRNA oligonucleotides targeting *HOXB7* (*siHOXB7*) or a single mixture with four different scrambled control siRNA oligonucleotides (*Scr*) was transiently transfected into S2-013 cells; 48 h later, the cells were incubated on fibronectin. Western blotting was performed using the indicated antibodies.

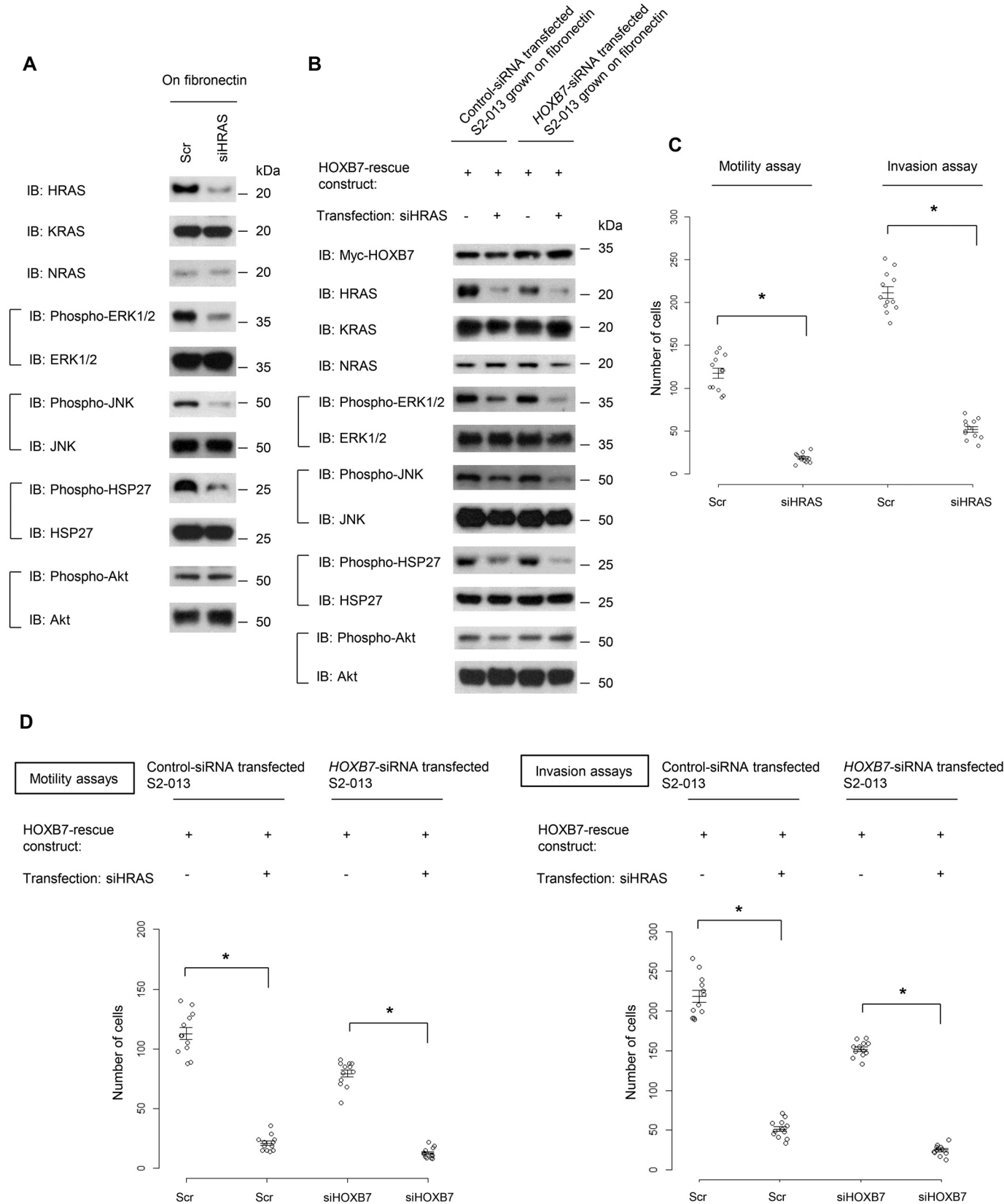
motility and two-chamber invasion assays using scrambled control siRNA-transfected S2-013 cells and *HOXB7* siRNA-transfected S2-013 cells with or without SP600125 pretreatment. Inactivation of JNK inhibited cell motility and invasion in scrambled control siRNA-transfected S2-013 cells (Fig. 13A). Transfection of a HOXB7 rescue construct into *HOXB7* siRNA-transfected S2-013 cells in

which JNK had been inactivated by SP600125 did not abrogate the changes to cell motility and invasiveness caused by the suppression of *HOXB7* and inactivation of JNK (Fig. 13A).

Transfection of *HSP27*-specific siRNAs into scrambled control siRNA-transfected S2-013 cells resulted in a decrease in cell motility and invasion (Fig. 13B). Transfection of a HOXB7-

rescue construct into S2-013 cells in which both HOXB7 and HSP27 had been suppressed did not abrogate the changes to cell motility and invasiveness caused by the *HOXB7* siRNA and

HSP27 siRNA (Fig. 13B). These results indicated that JNK and HSP27 were necessary for the HOXB7-associated promotion of cell motility and invasiveness.



HOXB7 promotes cell motility and invasion

Discussion

Extensive local infiltration and metastasis are the main causes of death in PDAC (26). The present study showed the role of HOXB7 in the promotion of motility and invasiveness through HOXB7/ERK1/2 signaling.

HOX genes encode transcription factors that are characterized by a highly conserved trihelical homeodomain that binds to specific DNA sequences (27, 28). Furthermore, HOXB7 is a *bona fide* target of microRNA-196b (miR-196b), and in turn, VEGF is a downstream transcript regulated by HOXB7 (29). The miR-196b/HOXB7/VEGF pathway plays an important role in the progression of cell growth, clonogenicity, migration, and invasion in cervical cancer (29). HOXB7 was also identified as the target of miR-337 (30). Overexpression of HOXB7 and down-regulation of miR-337 are seen in human PDAC tissues, and altered expression levels of HOXB7 and miR-337 are important for the invasion and metastasis of PDAC (31). These reports suggest that HOXB7 functions as a transcription factor to promote the invasiveness and metastatic properties of PDAC cells.

We previously reported that specific IGF2BP3-bound transcripts localized in cytoplasmic RNA granules, such as *ARF6* and *ARHGEF4*, are preferentially translated in membrane protrusions (12, 13). ARF6 and ARHGEF4 translated in membrane protrusions induce the further formation of membrane protrusions; consequently, IGF2BP3 promotes cell invasiveness and tumor metastasis (12, 13). The *HOXB7* transcript is one of the IGF2BP3-bound transcripts present in PDAC cells (12). Thus, our previous reports suggest that the local translation of *HOXB7* mRNA in the protrusions may be associated with cell invasion and metastasis. Adenomatous polyposis coli (APC) targets mRNAs to cell protrusions by forming APC-containing ribonucleoprotein complexes (29). APC-containing ribonucleoprotein complexes are concentrated in granules that probably contain many different transcripts (32). These complexes associate with the RNA-binding protein fused in sarcoma/translocated in liposarcoma (Fus/TLS), and Fus is required for the efficient translation of transcripts associated with APC and Fus in cell protrusions (33). Fus localized in RNA granules plays a role in local protein production from APC-containing ribonucleoprotein complexes. We confirmed *HOXB7* transcript assembly in cell protrusions by the use of immunofluorescence with RNA fluorescence *in situ* hybridization (data not shown); thus, showing that HOXB7 is accumulated in cell protrusions is important for elucidating the mechanism(s) behind the translational regulation of the *HOXB7* transcript.

The present study showed that HOXB7 was concentrated in cell protrusions and that knockdown of HOXB7 decreased peripheral rearrangement of the actin cytoskeleton in PDAC

cells cultured on fibronectin. Exogenously overexpressed HOXB7 was also accumulated in cell protrusions and significantly increased peripheral actin cytoskeletal rearrangement in *HOXB7* siRNA-transfected PDAC cells. The fact that the HOXB7 that remained after HOXB7 knockdown in *HOXB7* siRNA-transfected S2-013 and PANC-1 cells was localized to the cytoplasm of cell bodies and the nucleus (Fig. 3, A and B) suggests that HOXB7 accumulation at the cell membranes contributes to peripheral actin cytoskeletal rearrangement.

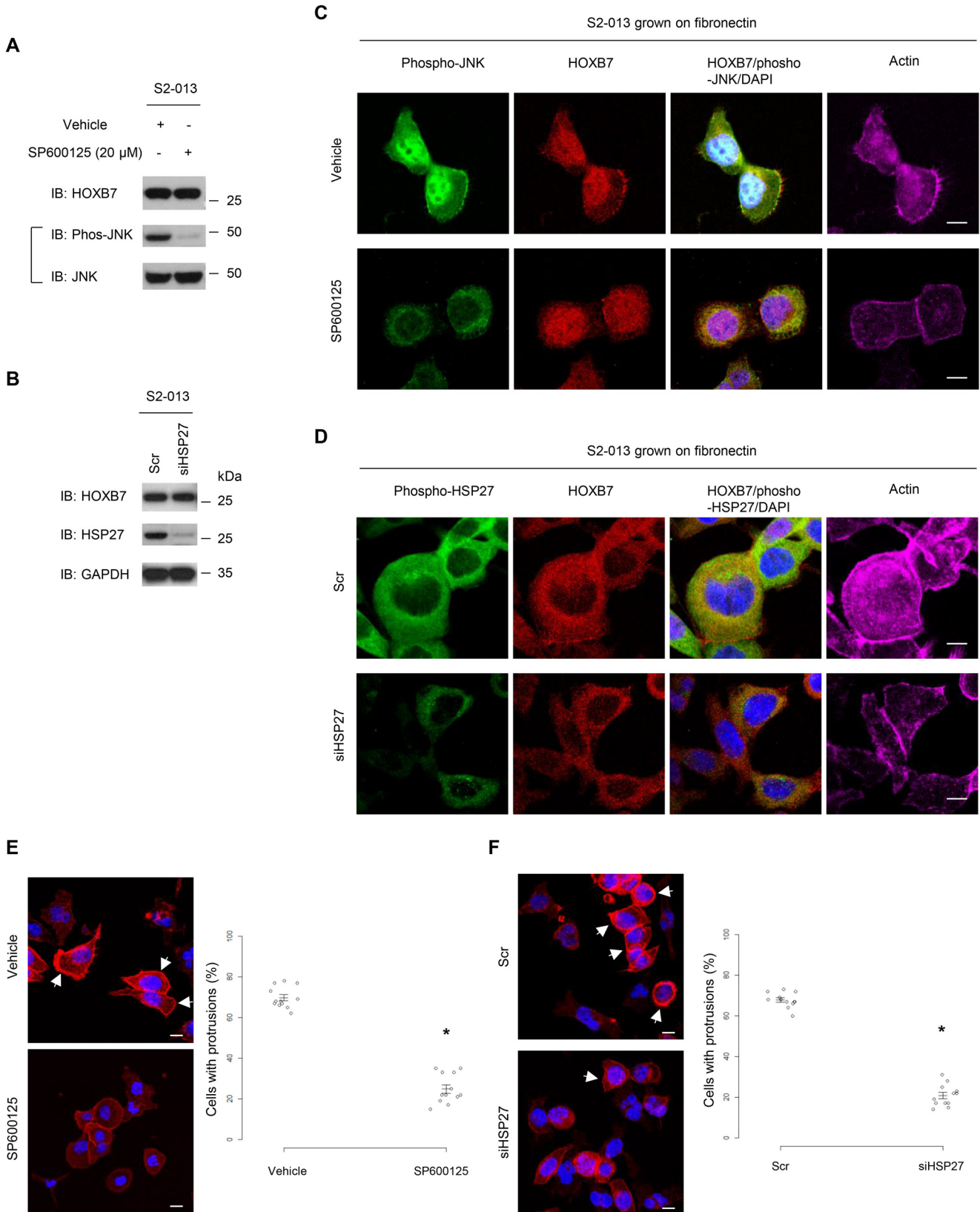
Dynamic actin remodeling processes at the leading edge of migrating cells are complex and involve increased rates of actin filament severing, capping, and dendritic branching (34). The migratory competence of tumor cells requires activation of the motile cycle, the first step of which is actin remodeling, which drives the formation of cell protrusions, defines the direction of migration, and initiates the growth of lamellipodia (35). Rho GTPases and their effectors are key intracellular signaling molecules that coordinate the cytoskeletal remodeling required for cell spreading, motility, and cell-shape changes (36). Among Rho GTPases, Rac1 stimulates the formation of lamellipodia and membrane ruffles to control cell motility (37). We previously reported that GTP-bound Rac1 accumulates in lamellipodia-like protrusions in PDAC cells and that treatment with the Rac1 inhibitor NSC23766 leads to a decrease in the level of GTP-bound Rac1 localized to the protrusions of PDAC cells (17). NSC23766 inhibits lamellipodia formation and the motility and invasiveness of PDAC cells (17). Nevertheless, the present study suggests that Rac1 signaling was not necessary for the HOXB7-associated promotion of cell motility and invasion of PDAC cells.

We showed that HOXB7 knockdown inactivated ERK1/2 and decreased the accumulation of phosphorylated ERK1/2 in the nucleus and the cytoplasm. The inactivation of ERK1/2 localized to the nucleus and the cytoplasm by treatment with the MEK inhibitor decreased cell protrusions (Fig. 7, B and C) and inhibited PDAC cell motility and invasion (Fig. 8A). Moreover, transfection of the HOXB7-rescue construct into S2-013 and PANC-1 cells in which HOXB7 had been suppressed and ERK1/2 phosphorylation had been blocked by the MEK inhibitor did not increase cell motility or invasion when compared with the corresponding U0126-untreated cells or the corresponding mock-transfected U0126-treated cells (Fig. 8, C and D). Once activated, ERK1/2 translocates to the nucleus and phosphorylates the Ets family of transcription factors and other targets (38). As a result of the downstream activation of cell cycle regulators, such as cyclin D, activation of the RAF/MEK/ERK signaling cascade has been associated with increased cell proliferation (39). GO analysis of global gene expression profiling indicated that the gene sets differentially expressed between

Figure 11. Up-regulated HRAS increased phosphorylated ERK1/2, JNK, and HSP27 and promoted cell motility and invasiveness. A, scrambled control siRNA oligonucleotides (*Scr*)-transfected S2-013 cells and siRNA oligonucleotides targeting *HRAS* (*siHRAS*)-transfected S2-013 cells were incubated on fibronectin. Western blotting (*IB*) was performed using the indicated antibodies. B, a Myc-tagged HOXB7-rescue construct was transfected into S2-013 cells that had been transfected with scrambled control siRNA or *HOXB7* siRNA with or without *HRAS* siRNA; 48 h later, the cells were incubated on fibronectin. Western blotting was performed using the indicated antibodies. C, transwell motility and invasion assays. Oligonucleotides (siRNAs targeting *HRAS* or scrambled siRNAs as the negative control) were transiently transfected into S2-013 cells; 48 h later, transwell motility and Matrigel invasion assays were performed. Migrating cells in four visual fields per group were scored. Data are derived from three independent experiments. Columns, mean; bars, S.E. *, $p < 0.02$ (Student's *t* test). D, a Myc-tagged HOXB7-rescue construct was transfected into S2-013 cells that had been transfected with scrambled control siRNA or *HOXB7* siRNA with or without *HRAS* siRNA; 48 h later, motility and two-chamber invasion assays were performed. Migrating cells in four fields per group were counted. Data are derived from three independent experiments. Columns, mean; bars, S.E. *, $p < 0.02$ (Student's *t* test).

HOXB7 siRNA-transfected S2-013 cells transfected with a HOXB7-rescue construct and incubated on fibronectin and treated without or with U0126 were significantly enriched in processes such as cell motility, migration, adhesion, and extra-

cellular matrix organization (Fig. 9B), which provides important clues regarding HOXB7/ERK1/2 signaling. These findings indicated that HOXB7-dependent motility and invasiveness are mediated, at least in part, by ERK signaling pathways.



HOXB7 promotes cell motility and invasion

Previous studies have shown that the RAF/MEK/ERK signaling cascade is affected by the KRAS oncogene in PDAC cells (40), and the RAS/ERK pathway is recognized as a driving force for tumor initiation and progression (41). Recent evidence indicates a role for the RAS/ERK pathway in cell invasiveness and metastasis; however, the mechanism remains unknown (42). Global gene expression profiling showed that the expression level of HRAS in HOXB7 siRNA-transfected S2-013 cells that were transfected with a HOXB7-rescue construct and subsequently incubated on fibronectin with U0126 was decreased in cells that were not incubated on fibronectin without U0126. Further analyses suggested that the up-regulated HRAS contributed to the HOXB7-mediated regulation system of ERK1/2 phosphorylation in PDAC cells. These results raised the possibility that HRAS might be an upstream molecule of HOXB7/ERK1/2 signaling. Galectin-1 contains an aprenyl-binding pocket, which interacts with the farnesyl group in HRAS, independent of lectin function (43). This interaction alters the orientation of the HRAS globular domain with respect to the plasma membrane and thereby regulates lateral segregation of HRAS and promotes MAPK signaling (44). Moreover, we showed that HRAS played roles in HOXB7-mediated PDAC cell motility and invasion. Further study of this unique property of the association of HRAS with HOXB7/ERK1/2 signaling may help to clarify the novel mechanism underlying the motility and invasiveness of PDAC cells.

The phosphorylation levels of ERK1/2, JNK, and HSP27 in HOXB7 siRNA-transfected S2-013 cells that were transfected with a HOXB7-rescue construct and subsequently incubated on fibronectin with U0126 were decreased in cells that were not incubated on fibronectin without U0126 (Fig. 7, A–C). Taken together with the result shown in Fig. 7D, this indicates that HOXB7 and phosphorylated ERK1/2 could be necessary for regulating the phosphorylation of JNK and HSP27 in PDAC cells. JNK is required for the maturation of actin-nucleating centers, the formation of filopodia and lamellipodia, and cell spreading (45). Spir is a JNK substrate that may function in regulation of the actin cytoskeleton and cell motility (46). Spir contains four WH2 domains and a C-terminal D domain. The WH2 domains of Spir bind to monomeric actin, and the D domain constitutes a docking site for JNK or ERK1/2 (46). HSP27 can be reversibly phosphorylated on three serine residues by the MAPK-activated kinases 2/3, which are themselves activated by phosphorylation through either the p38 or ERK signaling pathway, resulting in actin reorganization and cell migration (47, 48). These findings suggested that HOXB7 may be involved in regulating the phosphorylation levels of JNK and/or HSP27 through its linking with ERK1/2 and that this

HOXB7 pathway has a role in peripheral actin rearrangements and cell motility and invasiveness.

The findings presented in this study are supportive of pivotal roles for HOXB7 in the coordinated regulation of cortical actin changes; the functional significance of HOXB7, which mediates motility and invasiveness by activating ERK in PDAC cells, was established. The data presented herein indicated that inhibition of HOXB7 may be effective as a targeted molecular therapy, because any such therapy would limit the motility and invasiveness of PDACs.

Experimental procedures

Antibodies

Anti-HOXB7 antibody (H0291) was purchased from Sigma-Aldrich. Anti-RhoA (sc-418), anti-MYC proto-oncogene (sc-789), anti-JNK (sc-7345), anti-phosphorylated JNK (sc-6254), anti-HSP27 (sc-13132), and anti-phosphorylated HSP27 (sc-166693) antibodies were purchased from Santa Cruz Biotechnology, Inc. Anti-Rac1 (catalog no. 610650) and anti-Cdc42 (catalog no. 610929) antibodies were purchased from BD Transduction Laboratories (Palo Alto, CA). Anti-ERK1/2 (catalog no. 4697), anti-phosphorylated ERK1/2 (Thr-204/Tyr-187) (catalog no. 5726), anti-Akt (catalog no. 4691) and anti-phosphorylated Akt (Ser-473) (catalog no. 9271) antibodies were purchased from Cell Signaling (Grand Island, NY). Anti-HRAS (GTX116041) and anti-NRAS (GTX108598) antibodies were purchased from Gene Tex (Irvine, CA). Anti-KRAS antibody (12063-1-AP) was purchased from Proteintech (Chicago, IL).

Cell culture

The human PDAC cell line S2-013, which is a cloned subline of the SUIT-2 cell line derived from a liver metastasis, was obtained from Dr. T. Iwamura (Miyazaki Medical College, Miyazaki, Japan) (14). The human PDAC cell line PANC-1 was purchased from the American Type Culture Collection (Manassas, VA). All cells were grown in DMEM (Gibco) supplemented with 10% heat-inactivated FCS at 37 °C in a humidified atmosphere saturated with 5% CO₂. In selected experiments, cells were incubated with 30 μM U0126, a specific MEK inhibitor (Sigma-Aldrich), for 24 h or with 20 μM SP600125, a specific JNK inhibitor (Wako, Osaka, Japan), for 24 h.

Confocal immunofluorescence microscopy

Coverslips were coated with 10 μg/ml fibronectin (Sigma-Aldrich) for 1 h at room temperature. S2-013 cells were seeded on the fibronectin-coated glass coverslips and incubated for 5 h;

Figure 12. Association of JNK and HSP27 with peripheral rearrangements of the actin cytoskeleton. A, S2-013 cells were incubated on fibronectin with a JNK inhibitor (20 μM SP600125) or vehicle only. Cells were lysed, and equivalent amounts of whole-cell lysates were subjected to Western blotting (B) with the indicated antibodies. B, a single mixture with four different siRNA oligonucleotides targeting HSP27 (siHSP27) or a single mixture with four different scrambled control siRNA oligonucleotides (Scr) was transiently transfected into S2-013 cells. Western blotting of total cell lysates was performed using anti-HSP27 antibody. C, confocal immunofluorescence microscopy images. S2-013 cells treated as described in A were stained with anti-phosphorylated JNK antibody (green), anti-HOXB7 antibody (red), and phalloidin (violet). Blue, DAPI staining. Bars, 10 μm. D, confocal immunofluorescence microscopy images. S2-013 cells treated as described in B were stained with anti-phosphorylated HSP27 antibody (green), anti-HOXB7 antibody (red), and phalloidin (violet). Blue, DAPI staining. Bars, 10 μm. E and F, quantification of the data shown in C (E) and D (F). Actin filaments were labeled with phalloidin (red). Blue, DAPI staining. Four independent visual fields were examined via microscopic observation to count the number of cells that formed cell protrusions. Data are derived from three independent experiments. Columns, mean; bars, S.E. *, $p < 0.001$ compared with the corresponding controls (Student's *t* test). Arrows, peripheral actin structures in cell protrusions. Bars, 10 μm.

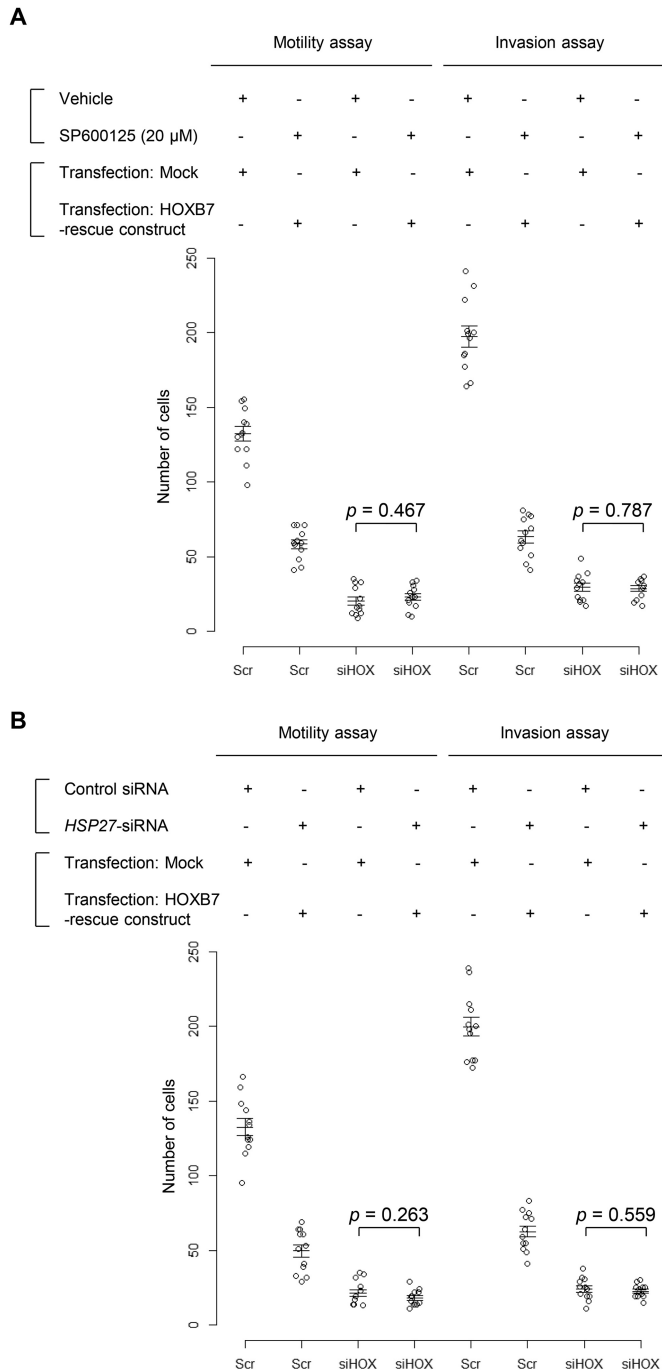


Figure 13. Association of HOXB7 with JNK and HSP27 in the motility and invasiveness of PDAC cells. A, a HOXB7-rescue construct was transfected into S2-013 cells that were transfected with scrambled control siRNA or *HOXB7* siRNA; 48 h later, the cells were treated with or without SP600125 and assayed using motility and two-chamber invasion assays. Migrating cells in four fields per group were scored. Data are representative of three independent experiments. Columns, mean; bars, S.E. B, a HOXB7-rescue construct was transfected into scrambled control siRNA or *HOXB7* siRNA-transfected S2-013 cells that had been transfected with or without *HSP27* siRNA; 48 h later, motility and two-chamber invasion assays were performed. Migrating cells in four fields per group were counted. Data are derived from three independent experiments. Columns, mean; bars, S.E.

the cells were then fixed with 4% paraformaldehyde, permeabilized with 0.1% Triton X-100, covered with blocking solution (3% bovine serum albumin in PBS), and then incubated with the primary antibody for 1 h. Next, Alexa 488- or Alexa 594-

conjugated secondary antibody (Molecular Probes, Carlsbad, CA) was used with or without Alexa 647- conjugated phalloidin (Cytoskeleton, Denver, CO). In some experiments, a commercial antibody-labeling technology (Zenon, Life Technologies) was used, according to the manufacturer's instructions, to conjugate green or red fluorophores to the primary antibodies. Each slide was visualized using a Zeiss LSM 510 META microscope (Carl Zeiss, Göttingen, Germany).

PDAC cells that formed cell protrusions, in which peripheral actin structures were accumulated, were counted by two blinded individuals (T. Shimizu and M. S.). Four independent visual fields were counted via microscopic observation to count the number of cells that formed cell protrusions. Data are derived from three independent experiments.

siRNA treatment

A single mixture with four different siRNA oligonucleotides targeting *HOXB7*, *HSP27*, or *HRAS* was purchased from Qiagen (FlexiTube GeneSolution siRNA GS3217, GS3315, and GS3265, respectively; Qiagen, Valencia, CA), and a single mixture with four different scrambled negative control siRNA oligonucleotides was obtained from Santa Cruz Biotechnology (catalog no. 37007). To examine the effects of these siRNAs on *HOXB7* and *HSP27* expression, S2-013 and PANC-1 cells, which express *HOXB7* and *HSP27*, were plated in 6-well plates. After 20 h, the cells were transfected with 80 pmol of each siRNA mixture in siRNA transfection reagent (Qiagen), according to the manufacturer's instructions. After incubation for 48 h, the cells were processed for Western blotting, transwell motility, or Matrigel invasion assays.

HOXB7-rescue construct

RT-PCR was used to amplify the entire coding sequence of the *HOXB7* cDNA. The resultant PCR product was subsequently inserted into a separate pCMV6-entry vector (Origene Technologies, Rockville, MD) bearing a C-terminal Myc-DDK tag. X-tremeGENE HP DNA Transfection Reagent (Roche Diagnostics, Penzberg, Germany) was used to transiently transfect target cells with the resultant *HOXB7*-rescue construct.

Immunoblot analysis of cell lysates

Cell pellets were resuspended in 20 mM Hepes (pH 7.4), 100 mM KCl, 2 mM MgCl₂, 0.5% Triton X-100, protease inhibitor mixture tablets (Roche Diagnostics), and a phosphatase inhibitor mixture (Nacalai, Kyoto, Japan). The bicinchoninic acid (BCA) assay was used to determine the protein concentration of each lysate; an aliquot of each lysate was then diluted with sample buffer (50 mM Tris, 2% SDS, 0.1% bromphenol blue, and 10% glycerol) to a final concentration of 1–2 μ g/ μ l and analyzed by SDS-PAGE and Western blotting.

Transwell motility assay

Cells (3.0×10^4) were plated in the upper chamber of BD BioCoat control culture inserts (24-well plates, 8- μ m pore size membrane; BD Biosciences). Serum-free culture medium was added to each upper chamber, and medium containing 5% FCS was added to the bottom chamber. Cells were incubated on the membranes for 12 h, and then four independent visual fields

HOXB7 promotes cell motility and invasion

were examined via microscopic observation to count the number of cells that had moved to the bottom chamber.

Matrigel invasion assay

A two-chamber invasion assay was performed to assess cell invasion (24-well plates, 8- μ m pore size membrane coated with a layer of Matrigel extracellular matrix proteins; BD Biosciences). Cells (4.0×10^4) suspended in serum-free medium were seeded into the upper chamber and allowed to invade toward a 5% FCS chemoattractant in the lower chamber. After a 20-h incubation period, four independent visual fields were examined via microscopic observation to count the number of cells that had moved to the bottom chamber.

Affinity precipitation using a GST-fused Rac1 interactive binding domain

The pGEX-6P1 plasmids encoding p21-activated kinase-CRIB domain or rhotekin were kindly provided by Dr. K. Johnson (University of Nebraska Medical Center, Omaha, NE). GST-binding fusion proteins were purified from transformed *Escherichia coli* using glutathione-Sepharose beads and were used for affinity precipitation in GST pull-down assays to estimate the activities of Rac1, Cdc42, and RhoA. Equal amounts of protein from each cell lysate that had been maintained in DMEM supplemented with 5% fetal bovine serum were incubated with 8 μ g of GST fusion protein, and the bound proteins were detected by Western blotting using anti-Rac1, anti-Cdc42, and anti-RhoA antibodies.

Determination of the patterns of protein phosphorylation

The relative protein phosphorylation levels of 38 selected proteins between scrambled control siRNA-transfected S2-013 cells and HOXB7 siRNA-transfected S2-013 cells and between HOXB7 siRNA-transfected S2-013 cells that were transfected with a HOXB7-rescue construct and subsequently incubated with 30 μ M U0126 or with vehicle for 24 h were obtained by profiling 46 specific phosphorylation sites using a Proteome Profiler human phosphokinase array kit ARY003 from R&D Systems (Minneapolis, MN) according to the manufacturer's instructions. Briefly, cells were rinsed with phosphate-buffered saline and solubilized in lysis buffer (1×10^7 cells/ml of lysis buffer) under continuous shaking at 4 °C for 30 min, and aliquots of the lysates were stored frozen at -80 °C. Membranes with spotted catcher antibodies were incubated with diluted cell lysates at 4 °C overnight. Thereafter, mixtures of biotinylated detection antibodies were added and incubated at room temperature for 2 h. Phosphorylated proteins were detected using a horseradish peroxidase-conjugated anti-mouse/rabbit antibody. Blots were then incubated with an enhanced chemiluminescence solution for 1 min and exposed.

Fractionation into nuclear and cytoplasmic subcellular fractions

Nuclear and cytoplasmic fractions were obtained from scrambled control siRNA-transfected and from HOXB7 siRNA-transfected S2-013 and PANC-1 cells grown on fibronectin using a LysoPure nuclear and cytoplasmic extractor kit (Wako) as described previously (49, 50).

Gene expression microarray analysis

HOXB7 siRNA-transfected S2-013 cells that were transfected with a HOXB7-rescue construct were incubated with or without 30 μ M U0126 for 24 h. Subsequently, these cells were grown on fibronectin for 5 h, following which the total RNA was extracted using a Qiagen RNeasy kit. The isolated RNA was quantified by measuring the absorbance at 260 nm, and purity was determined from the 260/280 nm absorbance ratio. Total RNA (100 ng) was processed with an Affymetrix GeneChip WT PLUS reagent kit (Affymetrix, Santa Clara, CA) for use in the microarray, according to the manufacturer's instructions (Kurabo, Osaka, Japan). The resultant single-stranded cDNA was fragmented and labeled with biotin and was then hybridized to an Affymetrix Human Gene 2.0 ST array (accession number of the GEO (<http://ncbi.nlm.nih.gov/geo/>): GPL16686). The arrays were washed, stained, and scanned using an Affymetrix 450 fluidics station and GeneChip scanner 3000 7G, according to the manufacturer's recommendations. The expression data were log₂-transformed, and expression values were generated using Expression Console software version 1.3 (Affymetrix) with default robust multichip analysis parameters. GO analyses were performed using GeneSpring GX version 14.0 (Agilent, Santa Clara, CA).

Semiquantitative RT-PCR

Total RNAs obtained from PDAC cells were subjected to reverse transcription with StrataScript reverse transcriptase (Agilent) and oligo(dT)₁₂₋₁₈ primers. We prepared appropriate dilutions of each single-stranded cDNA for subsequent PCR amplification; GAPDH mRNA was used as an internal quantitative control. The primer sequences used to amplify HRAS, KRAS, and NRAS are available on request.

Statistical analysis

StatFlex software version 6 (YUMIT, Osaka, Japan) and SAS software version 9.1.3 (SAS Institute, Cary, NC) were used for statistical analysis. Student's *t* test was used for the comparison of continuous variables. *p* values of <0.05 were considered to be statistically significant; all tests were two-tailed.

Author contributions—K. T. conceived and designed the experiments. M. T. and T. Shimizu performed the experiments. K. T. and M. S. coordinated the research and analyzed the data. K. T. wrote the manuscript with contributions from all authors. T. Saibara supervised the laboratory processes. K. T. obtained financial support. All authors read and approved the final manuscript.

Acknowledgments—We thank Hiroko Ohshita, Eriko Takahashi, Miki Nishikawa, and Hajime Kuroiwa for excellent technical assistance.

References

1. Krumlauf, R. (1994) Hox genes in vertebrate development. *Cell* **78**, 191–201
2. Chen, H., and Sukumar, S. (2003) Role of homeobox genes in normal mammary gland development and breast tumorigenesis. *J. Mammary Gland Biol. Neoplasia* **8**, 159–175
3. Topisirovic, I., Culjkovic, B., Cohen, N., Perez, J. M., Skrabanek, L., and Borden, K. L. (2003) The proline-rich homeodomain protein, PRH, is a

- tissue-specific inhibitor of eIF4E-dependent cyclin D1 mRNA transport and growth. *EMBO J.* **22**, 689–703
4. Caré, A., Silvani, A., Meccia, E., Mattia, G., Stoppacciaro, A., Parmiani, G., Peschle, C., and Colombo, M. P. (1996) HOXB7 constitutively activates basic fibroblast growth factor in melanomas. *Mol. Cell. Biol.* **16**, 4842–4851
 5. Naora, H., Yang, Y. Q., Montz, F. J., Seidman, J. D., Kurman, R. J., and Roden, R. B. (2001) A serologically identified tumor antigen encoded by a homeobox gene promotes growth of ovarian epithelial cells. *Proc. Natl. Acad. Sci. U.S.A.* **98**, 4060–4065
 6. Caré, A., Felicetti, F., Meccia, E., Bottero, L., Parenza, M., Stoppacciaro, A., Peschle, C., and Colombo, M. P. (2001) HOXB7: a key factor for tumor-associated angiogenic switch. *Cancer Res.* **61**, 6532–6539
 7. Wu, X., Chen, H., Parker, B., Rubin, E., Zhu, T., Lee, J. S., Argani, P., and Sukumar, S. (2006) HOXB7, a homeodomain protein, is overexpressed in breast cancer and confers epithelial-mesenchymal transition. *Cancer Res.* **66**, 9527–9534
 8. Chen, H., Lee, J. S., Liang, X., Zhang, H., Zhu, T., Zhang, Z., Taylor, M. E., Zahnow, C., Feigenbaum, L., Rein, A., and Sukumar, S. (2008) Hoxb7 inhibits transgenic HER-2/neu-induced mouse mammary tumor onset but promotes progression and lung metastasis. *Cancer Res.* **68**, 3637–3644
 9. Baumgart, M., Heinmöller, E., Horstmann, O., Becker, H., and Ghadimi, B. M. (2005) The genetic basis of sporadic pancreatic cancer. *Cell Oncol.* **27**, 3–13
 10. Nguyen Kovochich, A., Arensman, M., Lay, A. R., Rao, N. P., Donahue, T., Li, X., French, S. W., and Dawson, D. W. (2013) HOXB7 promotes invasion and predicts survival in pancreatic adenocarcinoma. *Cancer* **119**, 529–539
 11. Nakamura, T., Furukawa, Y., Nakagawa, H., Tsunoda, T., Ohigashi, H., Murata, K., Ishikawa, O., Ohgaki, K., Kashimura, N., Miyamoto, M., Hirano, S., Kondo, S., Katoh, H., Nakamura, Y., and Katagiri, T. (2004) Genome-wide cDNA microarray analysis of gene expression profiles in pancreatic cancers using populations of tumor cells and normal ductal epithelial cells selected for purity by laser microdissection. *Oncogene* **23**, 2385–2400
 12. Taniuchi, K., Furihata, M., Hanazaki, K., Saito, M., and Saibara, T. (2014) IGF2BP3-mediated translation in cell protrusions promotes cell invasiveness and metastasis of pancreatic cancer. *Oncotarget* **5**, 6832–6845
 13. Taniuchi, K., Furihata, M., and Saibara, T. (2014) KIF20A-mediated RNA granule transport system promotes the invasiveness of pancreatic cancer cells. *Neoplasia* **16**, 1082–1093
 14. Iwamura, T., Katsuki, T., and Ide, K. (1987) Establishment and characterization of a human pancreatic cancer cell line (SUIT-2) producing carcinoembryonic antigen and carbohydrate antigen 19–9. *Jpn. J. Cancer Res.* **78**, 54–62
 15. Deer, E. L., González-Hernández, J., Coursen, J. D., Shea, J. E., Ngatia, J., Scaife, C. L., Firpo, M. A., and Mulvihill, S. J. (2010) Phenotype and genotype of pancreatic cancer cell lines. *Pancreas* **39**, 425–435
 16. Taniuchi, K., Nishimori, I., and Hollingsworth, M. A. (2011) Intracellular CD24 inhibits cell invasion by posttranscriptional regulation of BART through interaction with G3BP. *Cancer Res.* **71**, 895–905
 17. Taniuchi, K., Yokotani, K., and Saibara, T. (2012) BART inhibits pancreatic cancer cell invasion by Rac1 inactivation through direct binding to active Rac1. *Neoplasia* **14**, 440–450
 18. Mackay, D. J., and Hall, A. (1998) Rho GTPases. *J. Biol. Chem.* **273**, 20685–20688
 19. Hall, A. (1998) Rho GTPases and the actin cytoskeleton. *Science* **279**, 509–514
 20. Lewis, T. S., Shapiro, P. S., and Ahn, N. G. (1998) Signal transduction through MAP kinase cascades. *Cancer Res.* **74**, 49–139
 21. Yip-Schneider, M. T., Lin, A., Barnard, D., Sweeney, C. J., and Marshall, M. S. (1999) Lack of elevated MAP kinase (Erk) activity in pancreatic carcinomas despite oncogenic K-ras expression. *Int. J. Oncol.* **15**, 271–279
 22. Yip-Schneider, M. T., and Schmidt, C. M. (2003) MEK inhibition of pancreatic carcinoma cells by U0126 and its effect in combination with sunitinib. *Pancreas* **27**, 337–344
 23. Mendoza, M. C., Er, E. E., and Blenis, J. (2011) The RAS-ERK and PI3KmTOR pathways: cross-talk and compensation. *Trends Biochem. Sci.* **36**, 320–328
 24. Huang, C., Jacobson, K., and Schaller, M. D. (2004) MAP kinases and cell migration. *J. Cell Sci.* **117**, 4619–4628
 25. Robitaille, H., Simard-Bisson, C., Larouche, D., Tanguay, R. M., Blouin, R., and Germain, L. (2010) The small heat-shock protein Hsp27 undergoes ERK-dependent phosphorylation and redistribution to the cytoskeleton in response to dual leucine zipper-bearing kinase expression. *J. Invest. Dermatol.* **130**, 74–85
 26. Ahrendt, S. A., and Pitt, H. A. (2002) Surgical management of pancreatic cancer. *Oncology* **16**, 725–734; discussion 734, 736–738, 740, 743
 27. Chang, C. P., Brocchieri, L., Shen, W. F., Largman, C., and Cleary, M. L. (1996) Pbx modulation of HOX homeodomain amino-terminal arms establishes different DNA-binding specificities across the HOX locus. *Mol. Cell. Biol.* **16**, 1734–1745
 28. Knoepfler, P. S., Bergstrom, D. A., Uetsuki, T., Dac-Korytko, I., Sun, Y. H., Wright, W. E., Tapscott, S. J., and Kamps, M. P. (1999) A conserved motif N-terminal to the DNA-binding domains of myogenic bHLH transcription factors mediates cooperative DNA binding with pbx-Meis1/Prep1. *Nucleic Acids Res.* **27**, 3752–3761
 29. How, C., Hui, A. B., Alajez, N. M., Shi, W., Boutros, P. C., Clarke, B. A., Yan, R., Pintilie, M., Fyles, A., Hedley, D. W., Hill, R. P., Milosevic, M., and Liu, F. F. (2013) MicroRNA-196b regulates the homeobox B7-vascular endothelial growth factor axis in cervical cancer. *PLoS One* **8**, e67846
 30. Li, Y., Zhang, M., Chen, H., Dong, Z., Ganapathy, V., Thangaraju, M., and Huang, S. (2010) Ratio of miR-196 s to HOXC8 messenger RNA correlates with breast cancer cell migration and metastasis. *Cancer Res.* **70**, 7894–7904
 31. Zhang, R., Zheng, S., Du, Y., Wang, Y., Zang, W., and Zhao, G. (2014) Levels of HOXB7 and miR-337 in pancreatic ductal adenocarcinoma patients. *Diagn. Pathol.* **9**, 61
 32. Mili, S., Moissoglou, K., and Macara, I. G. (2008) Genome-wide screen reveals APC-associated RNAs enriched in cell protrusions. *Nature* **453**, 115–119
 33. Yasuda, K., Zhang, H., Loisselle, D., Haystead, T., Macara, I. G., and Mili, S. (2013) The RNA-binding protein Fus directs translation of localized mRNAs in APC-RNP granules. *J. Cell Biol.* **203**, 737–746
 34. Bamburg, J. R., McGough, A., and Ono, S. (1999) Putting a new twist on actin: ADF/cofilins modulate actin dynamics. *Trends Cell Biol.* **9**, 364–370
 35. Eiseler, T., Döppler, H., Yan, I. K., Kitatani, K., Mizuno, K., and Storz, P. (2009) Protein kinase D1 regulates cofilin-mediated F-actin reorganization and cell motility through slingshot. *Nat. Cell Biol.* **11**, 545–556
 36. Ridley, A. J. (2001) Rho GTPases and cell migration. *J. Cell Sci.* **114**, 2713–2722
 37. Heasman, S. J., and Ridley, A. J. (2008) Mammalian Rho GTPases: new insights into their functions from *in vivo* studies. *Nat. Rev. Mol. Cell Biol.* **9**, 690–701
 38. Downward, J. (2003) Targeting RAS signalling pathways in cancer therapy. *Nat. Rev. Cancer* **3**, 11–22
 39. Pruitt, K., and Der, C. J. (2001) Ras and Rho regulation of the cell cycle and oncogenesis. *Cancer Lett.* **171**, 1–10
 40. Collisson, E. A., Sadanandam, A., Olson, P., Gibb, W. J., Truitt, M., Gu, S., Cooc, J., Weinkle, J., Kim, G. E., Jakkula, L., Feiler, H. S., Ko, A. H., Olshen, A. B., Danenberg, K. L., Tempero, M. A., Spellman, P. T., Hanahan, D., and Gray, J. W. (2011) Subtypes of pancreatic ductal adenocarcinoma and their differing responses to therapy. *Nat. Med.* **17**, 500–503
 41. Smakman, N., Borel Rinkes, I. H., Voest, E. E., and Kranenburg, O. (2005) Control of colorectal metastasis formation by K-Ras. *Biochim. Biophys. Acta* **1756**, 103–114
 42. Uekita, T., Fujii, S., Miyazawa, Y., Iwakawa, R., Narisawa-Saito, M., Nakashima, K., Tsuta, K., Tsuda, H., Kiyono, T., Yokota, J., and Sakai, R. (2014) Oncogenic Ras/ERK signaling activates CDCP1 to promote tumor invasion and metastasis. *Mol. Cancer Res.* **12**, 1449–1459
 43. Paz, A., Haklai, R., Elad-Sfadia, G., Ballan, E., and Kloog, Y. (2001) Galectin-1 binds oncogenic H-RAS to mediate RAS membrane anchorage and cell transformation. *Oncogene* **20**, 7486–7493

HOXB7 promotes cell motility and invasion

44. Prior, I. A., Muncke, C., Parton, R. G., and Hancock, J. F. (2003) Direct visualization of Ras proteins in spatially distinct cell surface microdomains. *J. Cell Biol.* **160**, 165–170
45. Kaltschmidt, J. A., Lawrence, N., Morel, V., Balayo, T., Fernández, B. G., Pelissier, A., Jacinto, A., and Martinez Arias, A. (2002) Planar polarity and actin dynamics in the epidermis of *Drosophila*. *Nat. Cell Biol.* **4**, 937–944
46. Otto, I. M., Raabe, T., Rennefahrt, U. E. E., Bork, P., Rapp, U. R., and Kerkhoff, E. (2000) The p150-Spir protein provides a link between c-Jun N-terminal kinase function and actin reorganization. *Curr. Biol.* **10**, 345–348
47. Rousseau, S., Houle, F., Landry, J., and Huot, J. (1997) p38 MAP kinase activation by vascular endothelial growth factor mediates actin reorganization and cell migration in human endothelial cells. *Oncogene* **15**, 2169–2177
48. O'Shaughnessy, R. F., Welti, J. C., Cooke, J. C., Avilion, A. A., Monks, B., Birnbaum, M. J., and Byrne, C. (2007) AKT-dependent HspB1 (Hsp27) activity in epidermal differentiation. *J. Biol. Chem.* **282**, 17297–17305
49. Turkson, J., Ryan, D., Kim, J. S., Zhang, Y., Chen, Z., Haura, E., Laudano, A., Sebt, S., Hamilton, A. D., and Jove, R. (2001) Phosphotyrosyl peptides block Stat3-mediated DNA-binding activity, gene regulation and cell transformation. *J. Biol. Chem.* **276**, 45443–45455
50. Svitkina, T. M., and Borisy, G. G. (1999) Arp2/3 complex and actin depolymerizing factor/cofilin in dendritic organization and treadmilling of actin filament array in lamellipodia. *J. Cell Biol.* **145**, 1009–1026